Aus der Medizinischen Klinik für Endokrinologie am Cardiovascular Metabolic Renal Research Center (CMR) der
Charité – Universitätsmedizin Berlin

DISSERTATION

Metabolic characterization and molecular alteration of *Aldh6a1*-deficient mice during diet-induced obesity

Metabolische Charakterisierung und molekulare Veränderung *Aldh6a1*-defizienter Mäuse unter diätinduzierter Adipositas

zur Erlangung des akademischen Grades
Doctor medicinae (Dr. med.)

vorgelegt der Medizinischen Fakultät
Charité – Universitätsmedizin Berlin

von

Rongwan Sun

Datum der Promotion: 25.06.2023

Table of Contents

List of Tables

List of Figures

List of Abbreviations

MetS	Metabolic syndrome
T2DM	Type 2 diabetes mellitus
DIO	Diet-induced obesity
GDM	Gestational diabetes mellitus
MODY	Maturity-onset diabetes of the young
GWAS	Genome-wide association studies
OSA	Obstructive sleep apnea
IR	Insulin resistance
IGT	Impaired glucose tolerance
IS	Insulin sensitive
FFA	Free fatty acid
TNF	Tumor necrosis factor alpha
IL-6	Interleukin 6
LFL	Low-density lipoprotein
Foxo1	Forkhead box protein O1
Srebp	Sterol regulatory element binding protein
CRP	C-reactive protein
Ras	Rennin-angiotensin system
CVD	Atherosclerotic cardiovascular disease
WHO	World Health Organization
BMI	Body mass index
VAT	Visceral adipose tissue
SAT	Subcutaneous adipose tissue
IL-8	Interleukin 8
IL-10	Interleukin 10
MCP	Monocytes chemoattractant protein
ALDH	Aldehyde dehydrogenase
ALDH6A1	Aldehyde dehydrogenase 6 family member 1
MMSDH	Methylmalonate semialdehyde dehydrogenase
3HIBA	3-hydroxyisobutyric acid

AIBA	Aminoisobutyric acid
NGT	Normal glucose tolerance
HCC	Hepatocellular carcinoma
ROS	Reactive oxygen species
NO	Nitric oxide
CcRCC	Clear cell renal cell carcinoma
AD	Alzheimer’s disease
ND	Normal diet
HFD	High fat diet
WD	Western diet
NMR	1H-magnetic resonance spectroscopy
LM	Labmaster
ipGTT	Intraperitoneal glucose tolerance test
ipITT	Intraperitoneal insulin tolerance test
EE	Energy expenditure
LV	Left ventricle
Val	Valine
Leu	Leucine
IIe	Isoleucine
PTT	Pyruvate tolerance test
BCAA	Branched amino acid
TCA	Tricarboxylic acid
OCR	Oxygen consumption rate
FCCP	Luo-carbonyl cyanide phenylhydrazone
EEG	Electroencephalogram
ECG	Electrocardiogram
OXPHOS	Oxidative phosphorylation
RER	Respiration exchange rate
IRS1	Insulin substrate receptor 1
Bckdha	Branched chain acid transfernatinase
Bcat	Branched chain acid transfernatinase
Scs	Succinate coenzyme A ligase
Glut 4	Glucose transporter type 4

BAT	Brown adipose tissue
QD	Quadriceps
Gas	Gastrocnemious
eWAT	Epididymal white adipose tissue
iWAT	Inguinal white adipose tissue
pWAT	Perirenalmetrial white adipose tissue

Abstract

Background: Visceral obesity is known to negatively correlate with insulin sensitivity (IS), contributing to metabolic syndrome (MetS) and type 2 diabetes (T2D). It has primarily been attributed to the insulin resistance (IR) of peripheral tissues and mitochondrial dysfunction in adipose tissue. Notably, previous studies indicated that Aldehyde dehydrogenase 6 family member A1 (ALDH6A1), an enzyme of valine catabolism, is associated with IR and mitochondrial oxidative pathways in obese patients with T2D. ALDH6A1 has been identified as a novel marker in the progression of T2D. Thus, it can be concluded that ALDH6A1 may regulate IS or oxidative phosphorylation (OXPHOS) pathways and therefore affect metabolism; however, no mouse model for ALDH6A1 has been described.

Methods: A constitutive *Aldh6a1*-deficient mouse model (*Aldh6a1*$^{-/-}$) generated via CRISPR-Cas9 technique was screened for tissue expression of *Aldh6a1*. Furthermore, male *Aldh6a1*$^{-/-}$ mice and wild type littermates (WT) were characterized during 12 weeks of normal diet (ND) or high-fat diet (HFD) to identify metabolic changes. Additionally, we measured their mitochondrial respiration and OXPHOS complexes *ex vivo* to evaluate mitochondrial function.

Results: In *Aldh6a1*$^{-/-}$ mice, fasting glucose concentration was improved. Moreover, HFD-fed *Aldh6a*$^{-/-}$ mice revealed a downregulation of genes involved in branched chain amino acid (BCAA) and glucose transport in skeletal muscle, accompanied by a general lean mass increase. In addition, improved oxidative phosphorylation in adipose tissue and increased hepatic mitochondrial flexibility were observed in *Aldh6a1*$^{-/-}$ mice under HFD. However, insulin sensitivity of peripheral tissues was not altered either on ND or HFD.

Conclusion: *Aldh6a1*$^{-/-}$ mice exhibited a slightly improved glucose metabolism during diet-induced obesity. However, against expectations, ALDH6A1 deficiency did not deteriorate the characteristics of obesity.

Zusammenfassung

Hintergrund: Adipositas korreliert mit der Abnahme von Insulinsensitivität (IS) und trägt zu Metabolischem Syndrom (MetS) sowie Typ-2-Diabetes (T2D) bei. Insulinresistenz (IR) der peripheren Gewebe sowie mitochondriale Dysfunktion im Fettgewebes wird primär der Adipositas zugeschrieben. Studien zeigten, dass ALDH6A1, ein Mitglied der Aldehyddehydrogenase 6-Familie A1 (ein Enzym im Valin-Abbau, eine entscheidende Rolle bei IR- und mitochondrialen oxidativen Signalwegen bei adipösen Patienten mit T2D spielen. ALDH6A1 wurde als möglicher, neuer Marker für eine Progression von T2D identifiziert. Daher könnte Aldh6a1 eine bedeutende Rolle bei Insulinsensitivität und den Signalwegen der oxidativen Phosphorylierung spielen und damit den Stoffwechsel beeinflussen Bisher wurde jedoch kein Mausmodell für ALDH6A1 beschrieben oder detailliert untersucht, welche Rolle ALDH6A1 im Stoffwechsel besitzt.

Methoden: Ein konstitutives *Aldh6a1*-defizientes Mausmodells (*Aldh6a1*$^{-/-}$), erzeugt mittels CRISPR-Cas 9, wurden auf die Expressionslevel von *Aldh6a1* in verschiedenen Geweben untersucht. Des Weiteren wurden männliche *Aldh6a1*$^{-/-}$ Mäuse und Wildtyp-Wurfgeschwister (WT) unter einer zwölfwöchigen Normal- (ND) und Hochfettdiät (HFD) charakterisiert, um metabolische Veränderungen zu identifizieren. Zusätzlich wurde deren mitochondriale Respiration und Schlüsselproteine der Atmungsketten *ex vivo* analysiert, um die Funktion der Mitochondrien und die oxidative Phosphorylierung unter *Aldh6a1* Defizienz zu beurteilen.

Ergebnis: Unsere Analysen ergaben, dass *Aldh6a1*$^{-/-}$ Mäuse eine verbesserte Blutglukose unter Fasten aufweisen. Weiterhin konnten wir zeigen, dass *Aldh6a1*$^{-/-}$ Mäuse unter HFD eine reduzierte Expression von Gene, die im verzweigtkettigen Aminosäurestoffwechsel (BCAA) und an der Regulation von Glukosetransportern im Muskel beteiligt sind, und eine erhöhte Zunahme von fettfreier Körpermasse haben. Darüber hinaus wurden bei *Aldh6a1*$^{-/-}$ Mäusen unter HFD eine verbesserte oxidative Phosphorylierung im Fettgewebe und eine erhöhte mitochondriale Flexibilität in der Leber entdeckt. Allerdings veränderten weder die HFD- noch die ND-Intervention die Insulinsensitivität peripherer Gewebe bei *Aldh6a1*$^{-/-}$ Mäusen.

Schlussfolgerung: ALDH6A1 zeigte ein verbessertes Stoffwechselprofil unter HFD-induzierte Adipositas. Entgegen der Vordatenlage verstärkte die ALDH6A1 Defizienz nicht die Folgen einer Adipositas.

1 Introduction

1.1 Metabolic disease

Metabolic pathways convert nutrients into energy to maintain cellular processes, tissue growth, cell survival and regeneration. The three branches of metabolism, represented by protein, lipid and carbohydrate, regulate whole-body energy balance. Metabolic characteristics often reveal the body's state of health and enable early lifestyle modification as same as avoidance of risk factors to prevent metabolic disease. Excessive nutrition in combination with reduced physical activity promotes metabolic disorders, such as obesity, T2D and metabolic syndrome.

1.1.1 Obesity

The excess body fat accumulation which characterizes obesity is measured according to the WHO by body mass index (BMI), waist circumference, skinfold thickness or bioimpedance. BMI is widely utilized by epidemiological studies. The WHO has issued the following classifications: BMI >25: overweight; BMI>30: obese[1]. 13% of adults were overweight or obese in 2016 and 39 million children were overweight in 2020[2]. Indeed, the trend of increasing rates continues and is predicted to rise by 2025 with an obesity prevalence of 18% for men and 21% for women[3]. Early identification and intervention are clearly suitable strategies for a better quality of health and life.

Fat deposition patterns are divided into visceral adipose tissue (VAT) that covers/surrounds inner organs and subcutaneous adipose tissue (SAT). Both VAT and SAT have significance for health consequences. In line with this, patients with multiple symmetric lipomatosis and lipedema who predominantly have SAT show better metabolic profiles[4,5], whereas accumulation of VAT is positively correlated with insulin resistance (IR), dyslipidemia, and inflammation[6]. VAT stores excess lipid predominantly through hypertrophy of adipocytes, while SAT regulates transcription factors, such as peroxisome proliferator-activated receptor-γ (PPARγ) and CCAAT/enhancer binding protein-α (C/EBPα), to promote differentiation of pre-adipocytes for hyperplasia[7]. As obesity progresses, white adipose tissue (WAT) fails to store surplus lipid, which is deposited ectopically.

The chronic inflammation state of obesity drives the development of IR which, in turn, decreases the anti-lipolytic effect of insulin on WAT, increasing FFAs in circulation. If

FFAs surpass the maximal β-oxidative capacity of WAT, fat accumulates in non-adipose tissues, such as liver, muscle, heart, and pancreas. Hypertrophic WAT becomes dysfunctional and inflammatory factors (TNF-α, interleukin 6 (IL6), IL-8 and monocyte chemoattractant protein (MCP-1)) are elevated, while anti-inflammatory factors such as IL-10 are reduced[8]. Dysfunctional WAT also upregulates the production of adipokines, such as leptin and resistin, while adiponectin release declines. High leptin levels have occasionally been identified as a risk factor for central obesity, hypertension and metabolic syndrome (MetS)[9,10], whereas adiponectin is thought to protect β-cells and preserve insulin sensitivity[11,12]. Low-grade inflammation impairs insulin signaling and is positively correlated with adipogenesis and remodeling[13]. Thus, obesity and its fat distribution are associated with adverse metabolic effects and contribute to developing T2D, and finally MetS.

1.1.2 Type 2 Diabetes (T2D)

Diabetes is a heterogeneous disease involving chronic hyperglycemia and the metabolic disorders of lipids, proteins and carbohydrates homeostasis[14]. T2D is strongly related to a history of family obesity and characterized by insulin deficiency or dysfunction[15]. Its common symptoms include thirst, hunger, passing more urine extreme fatigue, blurry vision, cut/bruises that are slow to heal and tingling/pain/numbness in the hands/feet. Examination shows hyperglycemia in the blood. As T2D progresses, it would trigger the micro- and macro-vascular complications, including coronary heart disease and peripheral neuropathy, long known for their contribution to CVD. In addition, diabetic foot and infectious diseases are also common in patients with elevated blood glucose, all of which combine to increase mortality from T2D[16].

A recent epidemiological survey estimated that 451 million people currently suffer from diabetes, which will increase to 693 million by 2045[17]. T2D accounts for around 90% of diabetes cases[18]. Differences in the prevalence of T2DM remain in the developed and developing world. Rates show modest increases in the United States and Japan, but much steeper changes in China and India (9.7% and 12.1%, respectively)[19,20]. Moreover, T2D rates are rising in children, teenagers and adolescents, following the trend of obesity in three groups)[21].

Some susceptibility loci have been identified by genome-wide association studies (GWAS)[22-28], and only 10% of variance in glycemic genetic traits could be correlated with T2DM[29]. Transcriptomic studies have revealed further genes related to T2D and

obesity[30]. there are some high-risk factors for T2D, such as obesity, incretin effects, changes in gut microbiota, immune dysregulation and inflammation, have exposed potential therapeutic targets[31]. Microbial dysbiosis may activate defense mechanisms, such as anti-microbial and oxidative stress exacerbating the pro-inflammatory state[32]. Vitamin D and K1 deficiency also adversely affect glycemia control[33] and insulin sensitivity (IS)[34]. However, obesity is the highest risk of developing T2D, especially visceral obesity. Obesity is always caused by sedentary lifestyles and energy-dense diets. In the clinic, most T2D patients are overweight and accompanied with IR, while their IR would be improved after healthy life control and exercise regularly[35,36].

In summary, T2D incidence has increased along with obesity. Obesity is not only the strongest risk factor for T2D but also contributes to developing MetS.

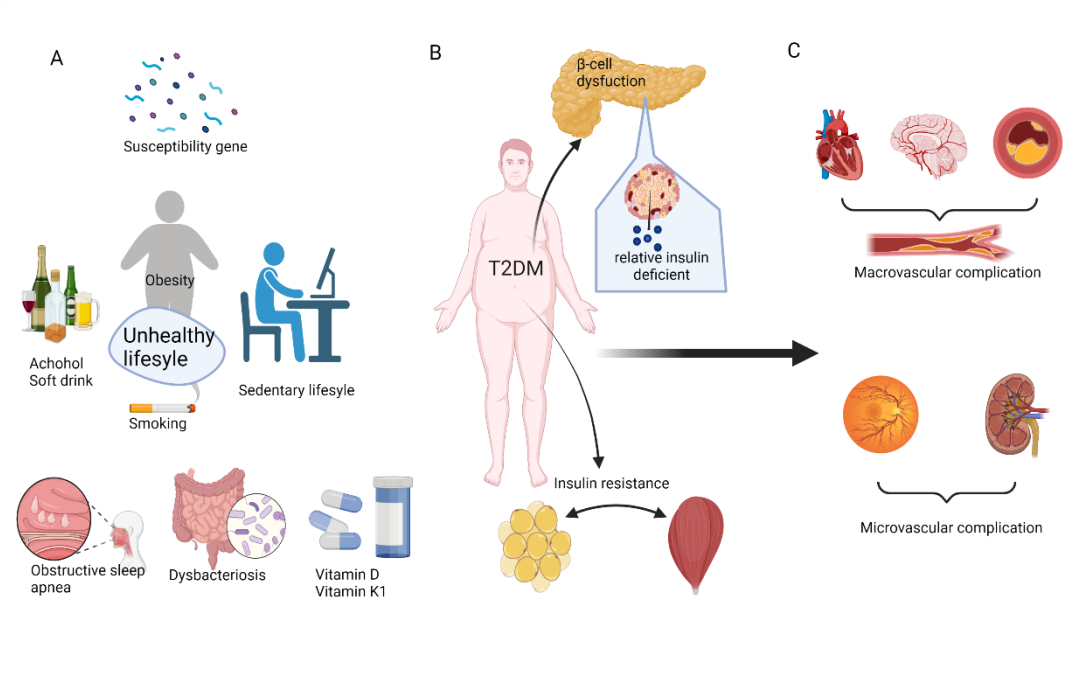

Figure 1 An overview of risk factors, mechanism and blood vessel complications of T2DM. Risk factors (A), mechanism (B), blood vessel complications (C). Created with BioRender.com.

1.1.3 Metabolic syndrome (MetS)

MetS, also known as syndrome X, is a metabolic disorder, including abdominal obesity, IR/T2D, dyslipidemia and hypertension. The rising numbers of MetS have attracted global attention, although the condition has diverse definitions (Tab. 1)[37]. The US National Health and Nutrition Examination Survey (NHNES) identified an increase in incidence from 25.3% to 34.2% in US adults, particularly among non-Hispanic white men (higher rates than in non-Hispanic black men)[38] and non-Hispanic black women (higher rates than in non-Hispanic white women[38]. The prevalence of MetS rose by 10.6% in urban China and by 5.3% in rural areas[39]. South-east Asia has, hitherto, a lower incidence of MetS, probably due to economic factors, but rates are catching up with those of the Western world.

Table 1 The three most popular definitions of MetS. IR: insulin resistance, BMI: body mass index, HDL: high-density lipoprotein. WHO: World Health Organization, NCEP ATPIII: National Cholesterol Education Program-Adult, IDF: international diabetes federation.

	WHO 1999	**NCEP ATPIII 2005**	**IDF 2006**
Criteria	Requirement (*) + two or more of the following	Three or more of the following:	Requirement (*) + two or more of the following:
Obesity	Waist/hip ratio >0.9 in me, >0.85 in women, or BMI >30 kg/m2	Waist >102 cm in men, >88 cm in women	*Waist >94 cm in men, >80 cm in women
Blood glucose	*IR or glucose >6.1 mmol/L (110 mg/dl), 2h glucose >7.8 mmol/L (140 mg/dl)	Glucose >5.6 mmol/L (100 mg/dl) or drug treatment	Glucose >5.6 mmol/L (100 mg/dl) or diabetes
HDL cholesterol	<0.9 mm/L (35 mg/dl) in men, <1.0 mml/L (40 mg/dl) in women	<1.0 mml/L (40 mg/dl) in men, <1.3 mml/L (50 mg/dl) in women or drug treatment	<1.0 mml/L (40 mg/dl) in men, <1.3 mml/L (50 mg/dl) in women or drug treatment
Triglycerides	<1.7 mml/L (150 mg/dl)	<1.7 mml/L (150 mg/dl) or drug treatment	<1.7 mml/L (150 mg/dl)
Blood pressure	>140/90 mmHg	>130/85 mmHg or drug treatment	>130/85 mmHg or drug treatment

Currently, the pathophysiology of MetS is complex and remains mostly unclear. Its etiology is based on a cluster of distinct pathologies associated with visceral obesity, IR (which often coincide) and dyslipidemia. The development of MetS is generally considered to be the interaction of IR with fatty acid flux[40]. The misfunction of insulin to inhibit lipolysis in adipose tissue drives the accumulation of free fatty acids (FFAs) in the circulation. A vicious cycle results from chronic inflammation induced by high FFAs which stimulate the production of tumor necrosis factor alpha (TNFα), interleukin 6 (IL-6), and increased levels of apolipoprotein B, which contributes to low-density lipoprotein (LDL) generation and indirectly aggravates IR[41]. Pancreatic β cells compensate for IR in liver and peripheral tissues by an increased output of insulin and the resulting hyperinsulinemia promotes the expression of transcription factors, i.e, forkhead box protein o1 (Foxo1) and sterol regulatory element binding protein (Srebp-1), which contribute to hepatic steatosis and hypertriglyceridemia[42]. Excessive FFAs are lipotoxic to pancreatic β cells and contribute to the development of T2D and hyperlipidemia. Adipose tissue secretes a range of cytokines, including IL-6, TNFα, adipokines, adiponectin and leptin. Increasing IL-6 drives the production of C-reactive protein (CRP) and fibrinogen, leading to the prothrombotic state[43], while TNFα induces inactivation of the insulin receptor and reduces adiponectin secretion[44]. Thus, the progression of obesity reduces the production of the anti-inflammatory and anti-atherogenic, adiponectin, whereas leptin levels increase. The abundance of pro-inflammatory cytokines, in combination with IR, contributes to the activation of the rennin-angiotensin system (Ras), leading to hypertension and cardiovascular disease (CVD)[45].

1.2 The correlation of obesity between MetS and T2D

Central obesity is known to contribute to T2D and correlate with MetS following a compensation period of hyperinsulinemia and a decompensation period of hyperglycemia. During compensation, WAT releases inflammatory factors and adipokines promoting IR in liver and peripheral tissues. Thus, insulin fails to inhibit WAT lipolysis and plasma FFAs further impairing insulin signaling. Hepatic insulin clearance is downregulated by impairment of CEACAM1[46] and the pancreas secretes higher, compensatory amounts of insulin. Pancreatic lipotoxicity plus islet inflammation due to $CD68^+$ and $CD11^+$ macrophages can lead to a drop in insulin secretion[47]. The point at which pancreatic com-

pensation fails to maintain euglycemia marks the commencement of the decompensation period and development of T2D.

1.3 Branched-chain amino acids (BCAA) and insulin resistance in obesity or T2D

There is an increasing awareness of the crucial role of branched-chain amino acids (BCAAs) dysfunction as potential biomarkers for development of obesity-induced diseases like MetS, T2D, and CVD[48,49].

BCAAs, including valine, leucine and isoleucine, account for 35-40% of the essential amino acid content of muscle protein in mammals and humans[50]. The interplay of hyperlipidemia and BCAA dysfunction may contribute to obesity and T2D, and elevated circulatory BCAAs have been identified as their predictors[51,52]. Indeed, mice fed a diet low in BCAA exhibit lower body weight, fat gain and higher energy expenditure[53]. Furthermore, mice during diet-induced obesity revealed improved body composition, glucose tolerance and insulin sensitivity if dietary Isoleucine or valine were restricted, although leucine restriction had no effect[54]. Intermediates of BCAA catabolism, including glutamine, alanine, 3HIBA[55], and C3/C5 acylcarnitines[56], are known to related to insulin action in obesity[57,58] , and a potential mechanism is the overactivation of the mTOR-S6K1 pathway, which inhibits IRS-1 and causes a negative feedback loop in obese individuals[59-61]. Further investigations are required to fully elucidate the mechanisms involved.

1.4 Aldehyde dehydrogenase 6 family member A1 (*Aldh6a1*)

Members of the aldehyde dehydrogenase (ALDH) superfamily play a critical role in protecting cells against the cytotoxic and carcinogenic effects of aldehydic compounds[62]. Aldehyde dehydrogenase 6 family member A1 (*Aldh6a1,* UniProtKB-Q02252) is located on chromosome 14q24 and encodes the enzyme methylmalonate semialdehyde dehydrogenase (MMSDH, OMIM: 614105) which catalyzes the irreversible oxidative decarboxylation of malonate and methylmalonate semialdehydes to acetyl-CoA and propionyl-CoA during valine and pyrimidine catabolism. The enzyme is abundant in rat kidney, liver, heart, muscle, and brain, and the mRNA expression of kidney is higher than liver[63]. Clinical MMSDH deficiency is characterized by homozygous or compounds heterozy-

gous mutation of the *Aldh6a1* gene[64-67], although additional homozygous variants have also been identified[68].

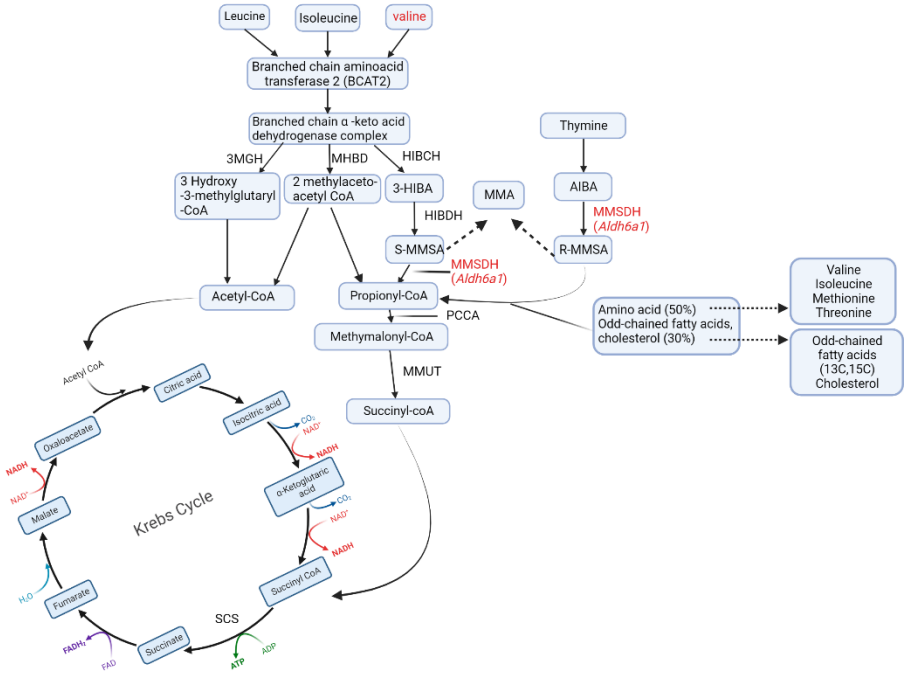

Figure 2 Overview of branched chain amino acid catabolism (BCAA) and Aldh6a1 function. 3MGH: 3-methylglutaconic acid, MHBD: 2-methyl-3-hydroxybutyryl-CoA dehydrogenase, HIBCH: 3-hydroxyisobutyrate dehydrogenase, 3-HIBA: 3-hydroxyisobutyric acid, HIBDH: hydroxyisobutyrate dehydrogenase, AIBA: aminoisobutyric acid, MMSA: methylmalonic semialdehyde, MMSDH: methylmalonate semialdehyde dehydrogenase, PCCA: propionyl-CoA carboxylase, MMUT: methylmalonyl-CoA mutase, SCS: succinyl-CoA synthetase. (Created with BioRender.com)

1.4.1 Studies investigating valine metabolism show opposing effects

Aldh6a1 is crucial for valine and thymine catabolism, producing propionyl-CoA, which enters the TCA (tricarboxylic acid) cycle. The catabolites of valine and thymine include 3-hydroxyisobutyric acid (3-HIBA) and aminoisobutyric acid (AIBA). Increased BCAA catabolic flux leading to elevated 3-HIBA has been shown to increase trans-endothelial FA import into muscle[55]. The knockdown of enzymes involved 3-HIBA formation causing WAT and BAT lipid accumulation[69]. Supraphysiological 3-HIBA treatment has been shown to inhibit mitochondrial oxidation and glycolytic metabolism in myotubes[70], while AIBA stimulates hepatic fatty acid β-oxidation and WAT browning, which also are nega-

tively related to cardiometabolic risk factors[71]. Therefore, it seems that intermediates of valine have opposing effects on the metabolic profile.

1.4.2 The clinical case reports, related diseases and research outcomes of *ALDH6A1* mutation

MMSDH deficiency is a rare autosomal recessive disease. To date, 7 case reports of patients with *ALDH6A1* mutation have been published. An overview of clinical parameters and treatments are summarized here (Tab. 2). In 1985, a mutation in the MMSDH coding region changing arginine to glycine was identified in a 3-week-old boy with higher urinary excretion of 3-hydroxypropionic acid, 2-hydroxymethyl butyric acid, 2-ethylhydracrylic acid, β-alanine and 3-amino isobutyric acid being found[64]. Between 1991 and 2020, further cases of disparate *ALDH6A1* mutations were identified with strikingly different metabolic profiles, but all showed elevated urinary 3-HIBA, aminoisobutyric acid (AIBA) and β-alanine[65-67].

Table 2 Features of published MMSDH case reports. EEG: electroencephalogram; ECG: electrocardiogram; MRI: magnetic resonance imaging; OCR: oxygen consumption rate.

Case reports	Patients (age/sex)	Clinical manifestation	Brain development	Examination alterations	Treatment/ outcome
1985 Pollott et al.[64]	17 days Male	Diarrhea and vomiting	Normal	Urine: β-alanine ↑, 3-HIBA ↑, 3-AIBA ↑, 3-Hydroxypropionate ↑ 2-butyruc acid ↑; Plasma: methionine ↑	Low-methionine diet; Biotin, thiamin, hydrochloride, pyridoxine, folic acid and hydroxocobalamin treatment
1991 Ko et al.[72]	6 years Male	Vomiting, acidosis and dehydration	Failure to thrive; EEG: the persistent vertex spike discharge	Muscle biopsy: Type I (68%) >Type II (32%); Electron microscopy: glycogen ↑; ECG: hypertrophy; Echo: normal; Urine: lactate ↑, 3-HIBA ↑, 3-AIBA ↑; Plasma: creatinine ↑	Carnitine treatment; Protein restriction diet

1998 Roe et al.73	18 months Male (A); 20 months Male (B)	Recurrent emesis (A); Development delay (B)	Skull films; EEG, MRI: Normal (B)	Plasma: MMA ↑ (A); Urine amino acid, EEG, Skin fibroblasts: Normal (B)	Surgery (gut-malrotation and Meckel's diverticulum)
2001 Shield et al.65	Newborn Female	Microphthalmia with cataracts and hypotonia	MRI: Delayed myelination thin corpus callosum	Plasma: lactate ↑ Urine: 3-HIBA ↑ 3-Hydroxypropionate ↑	Protein restriction diet; carnitine supplementation
2012 Sass et al.66	12 months Male (A); Newborn Female (B)	Developmental delay (A); Microphthalmia with cataracts and hypotonia (B)	No examination reported	Urine: β-alanine ↑ 3-HIBA ↑, 3-AIBA ↑, 3-Hydroxypropionate ↑	Death: Hepatic encephalopathy (A)
2019 Aghajanpour et al.74	4 years male	Cardiac disease (mild dilatation of left ventricle and left atrium-mitral value regurgitation)	No examination reported	Urine: β-alanine ↑, 3-HIBA ↑, 3-Hydroxypropionate ↑; Plasma: Lactate, pyruvate, TC, TG↑	Valine restriction diet
2020 Dobrowolski et al.68	Newborn female	Weight loss, gastroesophageal reflux, mild hypotonia	MRI: normal	Plasma/urine: β-alanine ↑,3-HIBA↑, 3-AIBA ↑; Urine: 3-Hydroxypropionate ↑; Fibroblast cells: Basal OCR ↓, ATP production ↓; Superoxide in mitochondrial ↑	Valine restriction diet

Transcriptomic studies of VAT and SAT from obese women with normal glucose tolerance (NGT) or T2D implicated down-regulation of the acetyl-CoA network in the pathophysiology of T2D. Four novel genes involved in acetyl-CoA metabolism were shown to be linked to T2D and weight loss-related recovery: *ALDH6A1, ACAT1, ACACA* and *MTHFD1*[75]. Moreover, *ALDH6A1*, which is involved in oxidative phosphorylation, has been identified as a risk marker for T2D and obesity[76,77]. Diabetes is not only associated with increased circulating BCAAs[78,79] but also with those of the valine degradation prod-

ucts, 3-HIBA or ABIA[69]. Recently, lower *ALDH6A1* has been identified as a new marker of muscle IR[80]. *ALDH6A1* has also been linked to reactive oxygen species (ROS) and nitric oxide (NO) production, hepatocellular carcinoma (HCC), and renal cell carcinoma. *ALDH6A1* was identified as a cerebrospinal fluid (CSF) biomarker for Alzheimer's disease in mice and humans[81, 82, 83]. In conclusion, a clinical and potential biochemical phenotype has been assigned the MMSDH deficiency and there is evidence for the function of *ALDH6A1*. However, further investigations are still required to elucidate its role in IR and oxidative phosphorylation fully.

1.5 Hypothesis and objectives

Although ALDH6A1 has been described as an obesity/T2D risk gene, there is barely any information about its role in IS and oxidative phosphorylation during obesity and T2D. The contribution of ALDH6A1 to insulin resistance (IR) still needs to be clarified.

To investigate the metabolic features of Aldh6a1, we established an *Aldh6a1*-deficient mouse model (*Aldh6a1*$^{-/-}$) using CRISPR/Cas 9 in our lab. Our objectives were metabolic profile, IS and oxidative phosphorylation in *Aldh6a1*$^{-/-}$ mice. This involved characterization of expression in male and female tissues to evaluate the metabolic profiles in *Aldh6a1*$^{-/-}$ mice with high fat diet-induced obesity (DIO); It was further verified whether *Aldh6a1*$^{-/-}$ mice alter IS and mitochondrial oxidative phosphorylation (OXPHOS).

2 Methods

2.1 Materials

Table 3 Buffers

Buffer	Reagent	Final concentration
RIPA	NaCl	150mM
PH: 8	Tris	50mM
	Triton	1%
	Sodium deoxycholate	1%
	EDTA	5mM
	In H_2O	
10x Running buffer	Tris base	250mM
PH: 8.3	Glycine	1.92M
	SDS	2%
	In H_2O	
10x Transfer buffer	Tris base	250mM
	Glycine	1.92M
	SDS	2%
	In H_2O	
10x TBS	Tris Base	200mM
PH: 7.6	NaCl	1.5M
	In H_2O	
1x TBST	10x TBS	1x
	Tween 20	0.1%

Homogenization-buffer	Saccharose	250mM
	HEPES	20mM
	EDTA	1mM
KRBH buffer	HEPES	20mM
PH: 7.4	KH_2PO_4	5mM
	$MgSO_4$	1mM
	$CaCl_2$	1mM
	NaCl	136mM
	KCl	4.7mM

Table 4 Antibodies for Western blots

Antibody	**Source**	**Dilution**	**Catalog number**
ALDH6A1	Santa Cruz	1:1000, 5% BSA	Sc-365160
Beta-actin (β-actin)	Cell signaling	1:1000, 5% BSA	4970
Alpha-tubulin (α-Tubulin)	NEB	1:1000, 5% BSA	2144
GAPDH	Cell signaling	1:1000, 5% BSA	2118
Phosphorylated AKT Tyr403 (pAKT)	Cell signaling	1:1000, 5% BSA	9271
AKT	Cell signaling	1:1000, 5% BSA	9272
OXPHOS	Abcam	1:1000, 5% skim milk	Ab110413

Table 5 Primer sequence for RT-PCR.

Gene	Orientation	Sequence
Aldehyde dehydrogenase 6 family member 1(*Aldh6a1* PM)	Fwd	5-AGCCGTTGAGTCCTGCAAAC-3
	Rev	TCCCTTGTTCCAGTGTGATTAAC
Aldehyde dehydrogenase 6 family member 1(*Aldh6a1* HRM)	Fwd	5-TGTGTACCACTGCATCAGACA-3
	Rev	TGATGAGGAAGAGAAGGAGGA
=>genotyping		
Propionyl-Coenzyme A carboxylase, alpha (*Pcca*)	Fwd	5-TTCATACCAATGCCTAGTGGTGT-3
	Rev	GACAGCCTCATCCGCCATTTT
Methylmalonyl-Coenzyme A mutase (*Mmut*)	Fwd	5-TTTTTGCTATCGCCCCATTACC-3
	Rev	CCTCTGGGTTTTTGCCTTTCAG
Succinate-Coenzyme A ligase, ADP-forming (*Scs*)	Fwd	5-ACCCTTTCGCTGCATGAATAC-3
	Rev	CCTGTGCCTTTATCACAACATCC
Branched chain ketoacid dehydrogenase E1, alpha (*Bckdha*)	Fwd	5-CTCCTGTTGGGACGATCTGG-3
	Rev	CATTGGGCTGGATGAACTCAA
Branched chain aminotransferase 1 (*Bcat1*)	Fwd	5-CCCATCGTACCTCTTTCACCC-3
	Rev	GGGAGCGTGGGAATACGTG
Branched chain aminotransferase 2 (*Bcat2*)	Fwd	5-CAGCCACACTAGGACAGGTCT-3
	Rev	CAGCCTTGTTATTCCACTCCAC
Beta actin	Fwd	5-GCCAACCGTGAAAAGATGACC-3
(*β-actin*)	Rev	CCCTCGTAGATGGGCACAGT

Peptidylprolyl isomerase A	Fwd	5-TCAACCCCACCGTGTTCTTC-3
(*Ppia*)	Rev	CCAGTGCTCAGAGCTCGAAA
18S ribosomal RNA	Fwd	5-TTGACGGAAGGGCACCACCAG-3
(*18s*)	Rev	GCACCACCACCCACGGAATCG
Glucose-6phosphatase	Fwd	5-CGAGGAAAGAAAAAGCCAAC-3
(*G6pc*)	Rev	GGGACAGACAGACGTTCAGC
Peroxisome proliferator-activated receptor gamma (*Pparg*)	Fwd	5-CCCTGGCAAAGCATTTGTAT-3
	Rev	ACCTCTTTGCTCTGCTCCTG
Peroxisome proliferator-activated receptor alpha (*Ppara*)	Fwd	5-AGACCCTCGGGGAACTTAGA-3
	Rev	GTGGGGAGAGAGGACAGATG
Acetyl-CoA carboxylase 1	Fwd	5-TCAGTAACCTGGTGAAGCTGG-3
(*Acc1*)	Rev	TGGCGATAAGAACCTTCTCAATTA
Acetyl-CoA carboxylase 2	Fwd	5-ACAGAGATTTCACCGTTGCGT-3
(*Acc2*)	Rev	CGCAGCGATGCCATTGT
ATP Citrate Lyase	Fwd	5-CAGCCAAGGCAATTTCAGAGC-3
(*Acly*)	Rev	CTCGACGTTTGATTAACTGGTCT
Fatty Acid Synthase	Fwd	5-GGAGGTGGTGATAGCCGGTAT-3
(*Fasn*)	Rev	TGGGTAATCCATAGAGCCCAG
Erythroid derived 2	Fwd	5-TAGATGACCATGAGTCGCTTGC-3
(*Nrf2*)	Rev	GCCAAACTTGCTCCATGTCC
Kelch-like ECH-associated protein 1(*Keap1*)	Fwd	5-TGCCCCTGTGGTCAAAGTG-3
	Rev	GGTTCGGTTACCGTCCTGC

Hormonsensitive lipase	Fwd	5-AGCGGATCACACAGAACCTG-3
(*Hsl*)	Rev	CAGGTCACAGGAGATGAGCC
Carnitine palmitoyltransferase 1 (*Cpt1*)	Fwd	5-ACCTGGTGCTCAAGTCATGG-3
	Rev	CCATGACCGGCTTGATCTCTT
Glucose transporter type 4	Fwd	5-GGCTGTGCCATCTTGATGAC-3
(*Glut4*)	Rev	AAGACGTAAGGACCCATAGCAT
Insulin receptor substrate 1	Fwd	5-TCCCAAACAGAAGGAGGATG-3
(*Irs1*)	Rev	CATTCCGAGGAGAGCTTTTG
Peroxisome proliferator-activated receptor gamma coactivator 1 (*Pgc1*)	Fwd	5-CCCAGGCAGTAGATCCTCTTCAA-3
	Rev	CCTTTCGTGCTCATAGGCTTCATA
Forkhead box protein O1	Fwd	5-ATCACCAAGGCCATCGAGAG-3
(*Foxo1*)	Rev	GTGAAGGGACAGATTGTGGC

2.2 Animals

Aldh6a1-deficient (*Aldh6a1*$^{-/-}$) experiments were conducted according to institutional ethical guidelines and approved by LAGeSo (Landesamt für Gesundheit und Soziales) Berlin under T 0180/16, T-CH19/21 and G 0160/19.

The *Aldh6a1*-deficient mice were generated by CRISPR/Cas 9 technology on a C57BL/6J mice background. Heterozygous mice were bred in the FEM to obtain WT and *Aldh6a1*$^{-/-}$ littermates. For experiments, mice were transferred to our animal facility and housed (2-3/cage) with a 12-hour light-dark cycle, controlled temperature (21.5 ± 1.5°C), with food and water *ad libitum,* and regular bedding changes. The diets were the normal maintenance chow (ND, sniff R/M GmbH) and high fat (HFD: D12492; Research Diets, with 60% kcal fat and 20% kcal carbohydrate).

2.3 In vivo metabolic experiments

2.3.1 Experimental arrangement

8 to 11-weeks-old-mice (n = 10/group) were assigned to ND and HFD (60% kcal fat + 20% kcal carbohydrate; Research Diets) groups for 12 weeks with weekly food and drink intake measurements.

Body composition was determined monthly by ^{1}H-magnetic resonance spectroscopy (NMR) using a Minispec LF50 Body Composition Analyzer (Bruker BioSpin, Billerica, USA). Monthly facial blood samples were taken, and serum was isolated by centrifugation (Thermo Fisher Scientific, USA) and stored at -80°C. Plasma glucose was measured in duplicate (≤10%) with a Contour XT glucometer (Ascensia). After 12 weeks ND or HFD, indirect calorimetry and activity were evaluated with the TSE LabMaster System (LM, labmaster) for a mouse in an individual cage for 48h (12h adaption/36 h for analysis: 1 light phase and mean of two-night phases). Intraperitoneal glucose tolerance tests (ipGTT) and insulin tolerance tests (ipITT) were conducted at 14 and 15 weeks, respectively. Mice were sacrificed at 16 weeks and organs were harvested and stored at -80°C. The experimental protocol is presented in the flowchart below (Fig. 3).

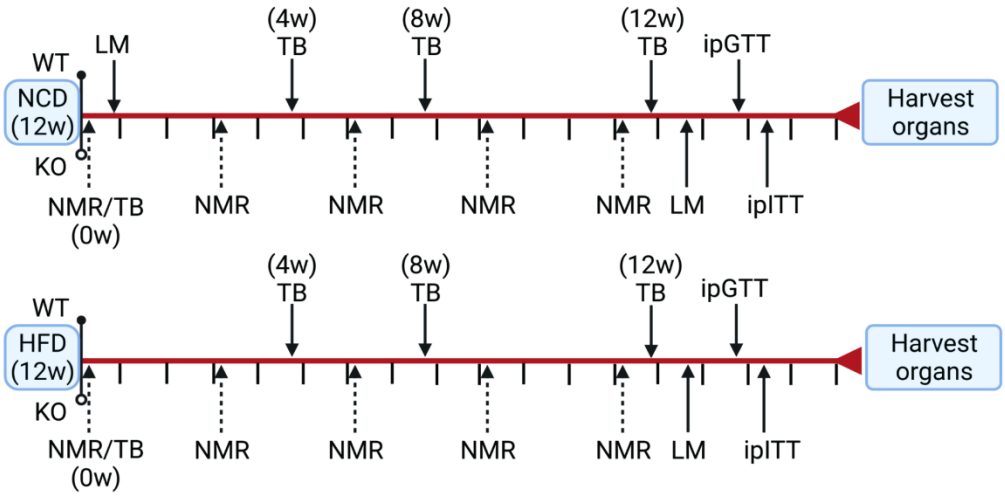

Figure 3 Schematic overview of the experiment design. Food and drink intake were recorded weekly. NMR was performed every 3 weeks and blood taken monthly. WT: wild-type mice, KO: *Aldh6a1*$^{-/-}$ mice, NCD: normal control diet, HFD: high fat diet, NMR: body composition, TB: taking blood, LM: metabolic cage (labmaster), ipGTT: intraperitoneal glucose tolerance test, ipITT: intraperitoneal insulin tolerance test.

2.3.2 Indirect calorimetry analysis (Labmaster)

All mice were allowed one day's adaption to the water bottles used before starting Lab master analysis. Each chamber had new bedding, food (ND, HFD) and water. The TSE LabMaster System (TSE Systems, Bad Homburg, Germany) was used to monitor metabolic parameters and perform 24 h analysis. Oxygen consumption and carbon dioxide production were measured at 30 min intervals and the respiratory exchange rate (RER) was calculated (ratio of CO_2 production: O_2 consumption). O_2 consumption, CO_2 production, energy expenditure (EE) and locomotor activity were adjusted for body weight.

2.3.3 Intraperitoneal glucose and insulin tolerance test

An intraperitoneal glucose tolerance test was performed after 12 weeks. Following a 5h fast, the basal tail vein blood glucose and body weight were measured, and serum was collected before an intraperitoneal bolus of glucose (HFD: 1 mg/g, ND: 2 mg/g) was injected. Blood glucose levels were measured at 0, 15, 30, 60 and 120 min. ipITTs were performed on 3 h fasted HFD mice at 14 weeks. Basal blood glucose and body weight were measured and fasting serum collected before an intraperitoneal bolus of 0.75 mU/g insulin was injected. Blood glucose levels were measured at 0, 15, 30, 45, 60, 90 and 120 min.

2.3.4 Sample preparation

The plasma and organs were collected after sacrificing the mice with CO_2 and stored at -80°C.

2.4 Ex vivo assays and measurements

2.4.1 Adipocytes isolation and lipolysis, insulin stimulation

Adipocytes were isolated from epididymal adipose tissue (eWAT) by collagenase digestion. eWAT was minced and digested for 30 min at 37°C in Krebs-Ringer HEPES buffer with 4.5 g/l glucose, 2% bovine serum albumin (BSA) and 1.0 mg/ml type I collagenase. The digested tissues were filtered through a 250 µm strainer to acquire floating adipocytes and washed once with KRBH buffer. Adipocytes were stimulated with 0/1/10/25/50 nM isoprenaline at 37°C, 300 rpm, and 3.5h for incubation. The sublayer of adipocytes was collected to measure non-esterified fatty acids (NEFA) levels.

2.4.2 Ex vivo insulin stimulation and glucose uptake in adipocytes

Adipocytes were deprived of substrates for 30 min. Adipocytes were stimulated with 4.5 g/L glucose, 10 nM/100 nM/1000 nM insulin for 15 min. Cooling RIPA was added instead of buffer for 30 min on ice and eventually adipocytes were harvested for protein extraction.
We performed *ex vivo* 2-DG uptake analysis in adipocytes with glucose or insulin stimulation (concentrations shown above) for 15 min. This was followed by collecting sublayer of adipocytes with ice-cold lysis buffer (NaOH: 50 mM) for 2-DG uptake measurement using liquid scintillation counting.

2.4.3 Ex vivo insulin stimulation in muscle.

Fresh SOLs (soleus) were fasted for 30 min, 37°C and stimulated with 100 nM insulin for 15 min. Cooling RIPA was added instead of buffer for 30 min on ice and eventually SOLs were harvested for protein extraction.

2.4.4 Tissue measurement (mitochondrial respiration in tissues)

Liver, eWAT, brown adipose tissue (BAT) and muscle were excised quickly, and biopsies of diameter 1.0mm (liver) or 1.5 mm (muscle, eWAT, BAT) were taken. Samples were placed in a 96-well seahorse plate in PBS and changed for assay medium before

measurement (DMEM 5030, pH 7.4, 2 mM glutamine, 2 mM glucose). The sensor plate with calibration buffer was incubated in CO_2 free incubator for 1h. A micro-BCA assay was used to measure protein for normalization. The oxygen consumption rate (OCR) was measured with an XF96 extracellular flux analyzer (Agilent). 5µM FCCP (Sigma) was used to measure maximal OCR, and then to calculate spare capacity (%) to evaluate the mitochondrial capability. 2.5µM antimycin A (complex III inhibitor, Sigma) and 2.5µM rotenone (complex I inhibitor, Sigma) were given to indicate non-mitochondrial respiration.

All data were normalized to the total protein content of each biopsy as determined by the Micro BCA Protein Assay Kit (Thermo Fisher Scientific).

2.5 Biochemical analysis

2.5.1 Real-time PCR

Quantitative real-time PCR was performed on a LightCycler 96 (Roche) with the SYBR green DNA PCR kit (Applied Biosystems). RNA was isolated from snap-frozen tissue samples using TRIzol reagent and DNA digested with DNase. An Aliquot of 1 mg RNA was transcribed into cDNAwith RevertAid Reverse Transcriptase. Relative fold changes in RNA were calculated by the $2^{-\triangle\triangle Ct}$ method with glyceraldehyde-3-phosphate dehydrogenase (*Gapdh*) and 18s ribosomal RNA (*18s)* as housekeeping genes. The primers for quantitative real-time PCR (RT-PCR) are shown (Tab. 5).

2.5.2 Western blot

Frozen tissues were homogenized in RIPA buffer (Tab. 3) using a Speedmill or tissue homogenizer. Loading samples were prepared by BCA Protein analysis. Following separation, the proteins were transferred onto nitrocellulose membrane, and blots were blocked with 5% skimmed milk in TBST for 1h at room temperature (RT). The blots with primary antibodies were incubated overnight at 4℃. Membranes were probed with HRP-conjugated secondary antibodies for 1h at RT, and incubated with imaging solution.

The blotting was achieved with the following antibodies (Tab. 4): anti-ALDH6A1, anti-β actin, anti-GAPDH, anti-α Tubulin, anti–phosphorylated AKT Tyr403, and anti-Akt). The protein signals were visualized using the Image Lab system.

2.5.3 Oxidative phosphorylation

Frozen tissues with homo-buffer (Tab. 3) were homogenized through a Speedmill or tissue homogenizer. The following steps are the same as for the Western blot, using total OXPHOS antibody-cocktail (Tab. 4).

2.5.4 Histology

Snap frozen liver specimens were embedded in O.C.T. Compound (Sakura) and 5-µm-thick sections were cut using a Jung Frigocut 2800E (Leica) and stained with Oil Red O for inspection using 20x magnification on a BZ-9000 microscope (Keyence). The mean percentage of Oil Red O-covered area was estimated with Image J (V1.52a).

2.5.5 Biochemical parameters in serum or tissue

Serum insulin levels were detected with a mouse insulin ELISA kit (Mercodia). A NEFA-HR (2) kit (FUJIFILM Wako Diagnostics, U.S.A.) and triglycerides Kit (Diagnostic Systems GmbH, Germany) were used to measure NEFAs and Triglycerides, respectively.

2.6 Statistical analysis

All data are presented as mean ± SEM. Normally distributed data were analyzed by Shapiro-Wilk test and equality of variance by Levene's test. The student's t-test or Welch's test or Mann-Whitney U test were performed to compare the differences between two groups according to data distribution. Two-way ANOVA was used for multiple comparison (Bonferroni correction). The threshold for statistical significance was $p < 0.05$. Statistical analyses and graphs were completed using SPSS 27 (IBM, New York, NY, USA) and Graph Pad Prism 9 (Graph Pad Software, La Jolla, CA).

3. Results

3.1 *Aldh6a1* expression in mice

First, we determined ALDH6A1 protein abundance in WT male and female mice to evaluate its expression in relevant metabolic tissue. The high abundance of ALDH6A1 protein was found in heart, liver, muscle, BAT, pancreas and WAT of female, and heart, muscle, BAT, liver, kidney and WAT of male adult mice (Fig. 4C). As previous case reports showed more males (6) than females (3) with ALDH6A1 mutation (Tab. 2), and taking into consideration potential changes of the estrous cycle and gonadal hormones[84], we decided to use male mice for further experiments.

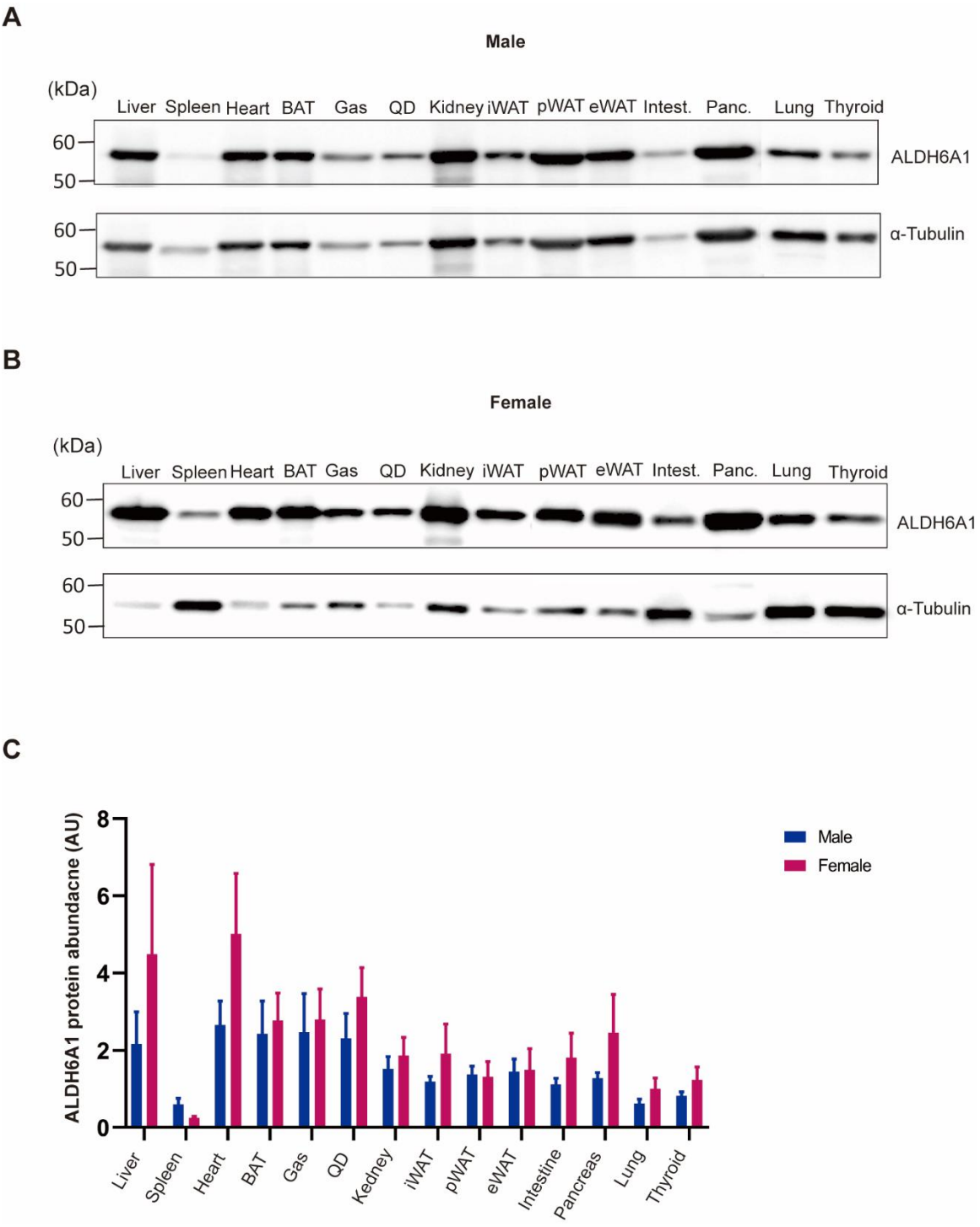

Figure 4 The ALDH6A1 protein abundance in different tissues between male and female mice. The protein abundance in different tissues were determined by Western blot, and the signal intensities are presented and normalized to α-tubulin (male: n = 4, female: n = 5). Representative Western blots of ALDH6A1 in male (A) and female mice (B). (C)Summary of ALDH6A1 protein abundance in both groups of mice. Statistical testing, Mann-Whitney test. BAT: brown adipose tissue, QD: quadriceps, Gas: gastrocnemius, eWAT: epididymal white adipose tissue, iWAT: inguinal white adipose tissue, pWAT: perirenalmetrial white adipose tissue, Intest.: intestine, Panc.: pancreas.

To verify the successful deletion of the *Aldh6a1* gene (*Aldh6a1*$^{-/-}$ mice) via CRISPR/Cas9 on RNA and protein levels, *Aldh6a1* expression was assessed in liver, muscle, eWAT, heart, kidney and BAT via qPCR and Western blot. As expected, *Aldh6a1* mRNA was significantly decreased in *Aldh6a1*$^{-/-}$ mice relative to WT controls ($p < 0.03$, Figure 5A). Consistently, ALDH6A1 protein was reduced by at least 95% in the examined tissues of *Aldh6a1*$^{-/-}$ mice ($p < 0.004$, Fig. 5B-E).

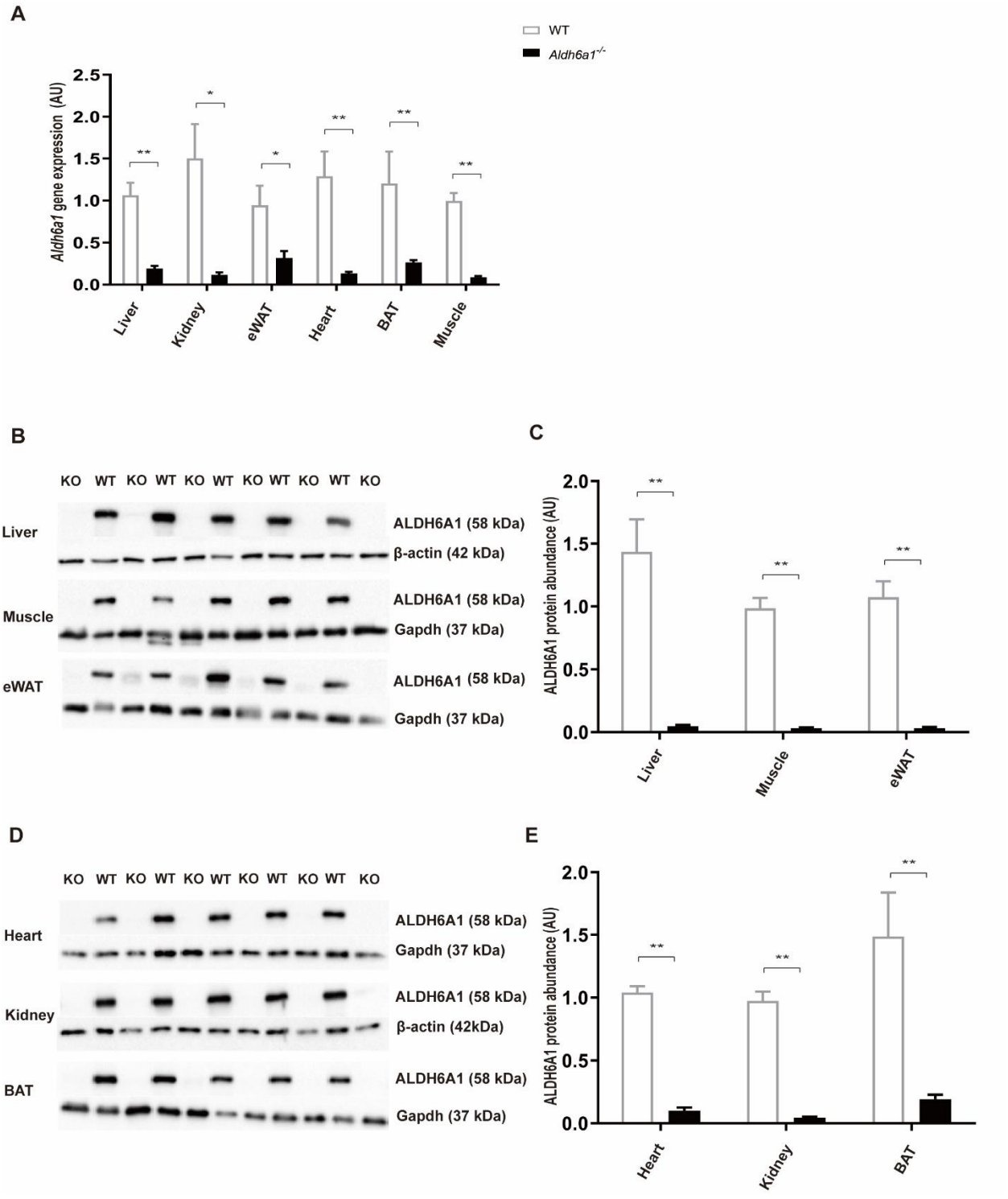

Figure 5 RNA and protein expression in *Aldh6a1*$^{-/-}$ mice. (A) *Aldh6a1* mRNA expression in liver, QD, eWAT, heart, kidney, and BAT between wild type (WT) and *Aldh6a1*$^{-/-}$ mice. Liver, heart, kidney were normalized to 18s and eWAT, BAT, QD to Ppia. Western blot analysis of ALDH6A1 from liver, QD, eWAT (B, C) and Heart, Kidney, BAT (D, E) in WT and *Aldh6a1*$^{-/-}$ mice. β-Actin and GAPDH were used as loading control. Values are presented as box with median and whiskers from minimum to maximum. n = 6/5, *p < 0.05, **p < 0.01. Statistical testing, Mann-Whitney test (A, C, E). AU: arbitrary units. KO: *Aldh6a1*$^{-/-}$, WT: wild type.

3.2 Body composition and intake of *Aldh6a1*$^{-/-}$ mice under dietary interventions

WT and *Aldh6a1*$^{-/-}$ mice were fed an ND or HFD for 12 weeks. The mice showed increased body weight regardless of genotype or diet effect (Fig. 6A, B), and became obese after 3-4 weeks during HFD intervention. No difference in body weight gain was found between WT and *Aldh6a1*$^{-/-}$ mice during the ND (Fig. 6A, left side) or HFD (Fig. 6B, left side). ND and HFD-fed *Aldh6a1*$^{-/-}$ mice had slightly reduced fat mass relative to WT mice, but no significant difference (Fig. 6C, D). Interestingly, *Aldh6a1*$^{-/-}$ mice on HFD showed more lean mass gain compared to the WT group ($p = 0.049$, Fig. 6F), but no effect with ND (Fig. 6E). There were no different observations in food (Fig. 6G) and water intake (Fig. 6I) between *Aldh6a1*$^{-/-}$ and WT mice on ND, while *Aldh6a1*$^{-/-}$ mice fed more on the HFD during the entire intervention ($p = 0.006$, Fig. 6H). Furthermore, during the HFD, *Aldh6a1*$^{-/-}$ mice also drank 22% more water ($p = 0.0003$, Fig. 6J).

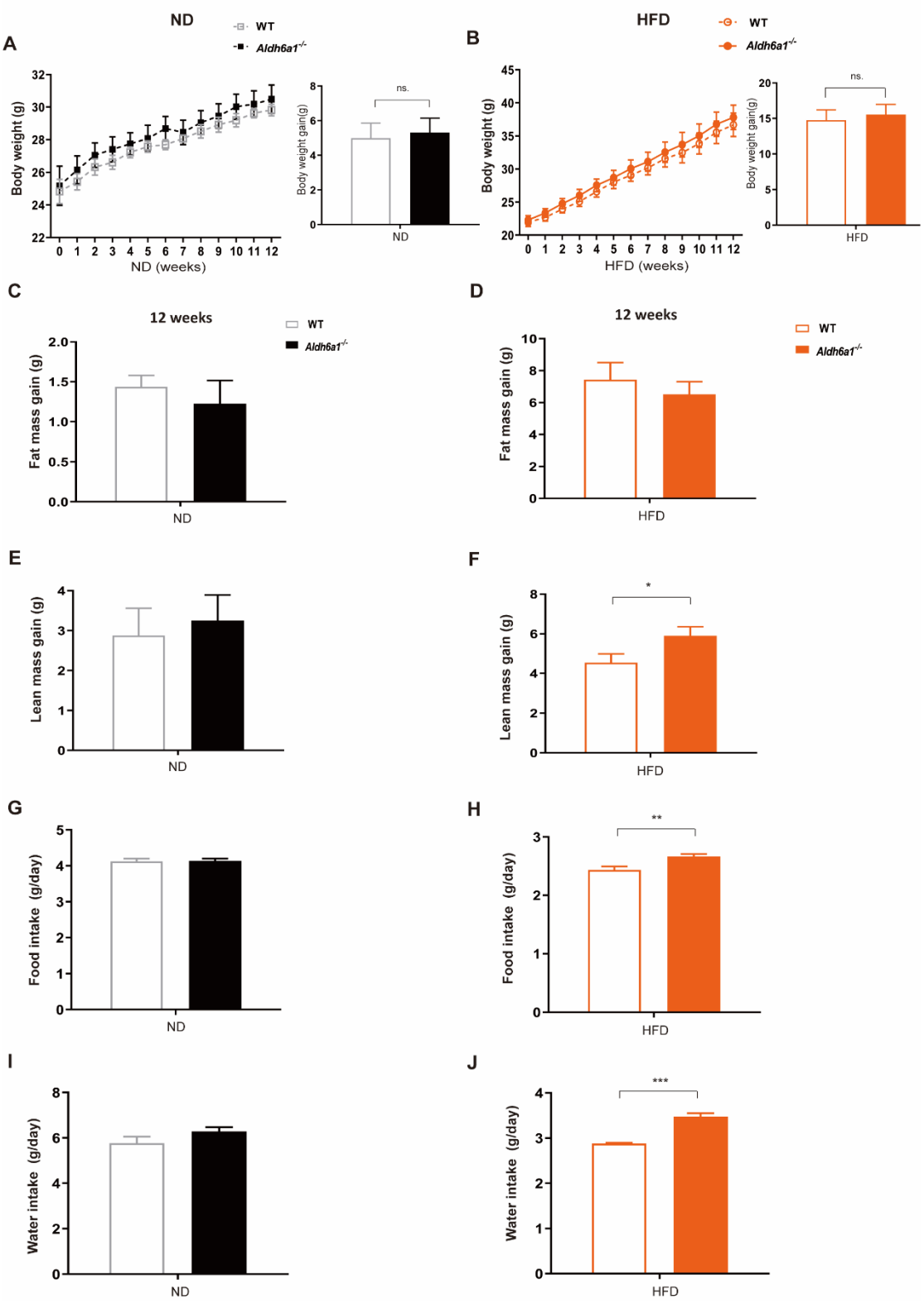

Figure 6 The body composition, food and water intake in WT and KO *Aldh6a1*$^{-/-}$mice with diets intervention. The development of body weight in each group over a period of 12 weeks with ND (A, right side: the corresponding body gain relative to baseline) and HFD (B, right side: the corresponding body gain relative to baseline), ND: 10/9, HFD: n = 10/10. Fat gain (C, D) and lean gain (E, F) measured after 12 weeks-ND/HFD feeding in mice relative to 0 weeks. Mean daily

food intake (G, H) and water intake (I, J) in mice over entire ND and HFD intervention. $^{*}p < 0.05$; $^{**}p < 0.01$ and $^{***}p < 0.001$. Values are presented as mean ± SEM. Statistical testing, two-tailed unpaired Student's t-test (A-J).

3.3 Metabolites activity of *Aldh6a1* deficient mice fed a HFD

We performed indirect calorimetry analysis to explore the energy expenditure (EE) and activity of *Aldh6a1*$^{-/-}$ mice. At baseline before starting dietary interventions energy expenditure (Fig. 7A) and activity (Fig. 7B) were similar between genotypes. After completion of the interventions, the HFD decreased RER because of the utilization of fat burning to support energy (Diet effect: F (1, 35) = 291.4, *d* = 8.047, Fig. 7C). Moreover, *Aldh6a1*$^{-/-}$ mice fed the ND showed an increased tendency of daily EE compared to WT mice, close to significance (p = 0.054, Fig. 7D), but there is no difference in mice with HFD intervention (Fig. 7E). No difference was evident in locomotor activity between WT and *Aldh6a1*$^{-/-}$ mice fed the ND (Fig. 7F), whether during the light phase or dark phase. While the activity of HFD-fed *Aldh6a1*$^{-/-}$ mice was higher in the light phase (p = 0.03, Fig. 7G) but similar during the dark phase and missed significance as mean over 24 h.
In summary, HFD caused lower RER in mice of both genotypes, however deficiency of *Aldh6a1* did not affect activity regardless of dietary intervention. Interestingly, ND-fed *Aldh6a1*$^{-/-}$ mice exhibited increased EE slightly relative to WT mice.

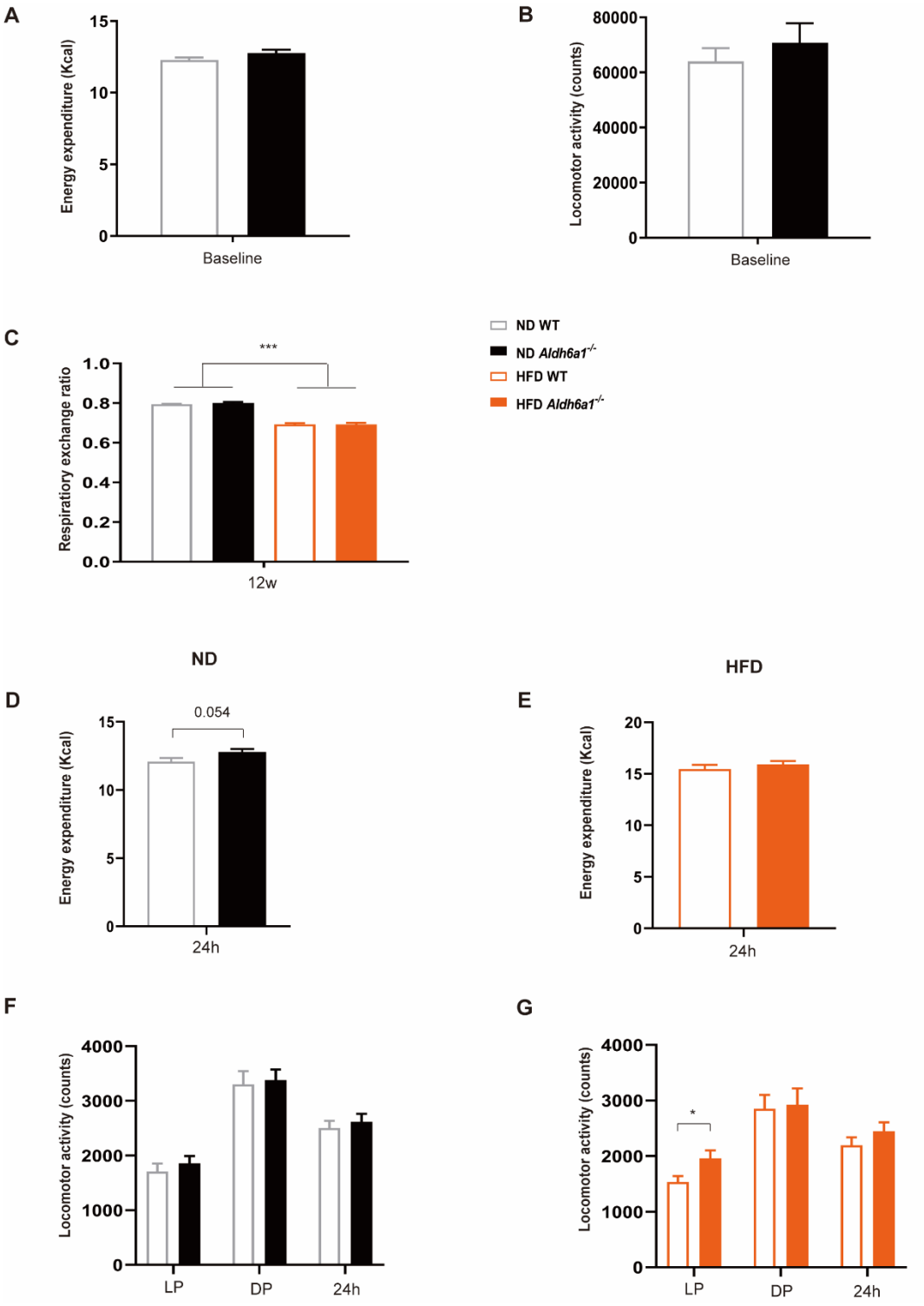

Figure 7 The respiration exchange ratio (RER), energy expenditure (EE) and physical activity in HFD- or ND-fed *Aldh6a1*$^{-/-}$ mice and WT littermates. Metabolic cage analysis was performed after 12 weeks of HFD, all mice were placed in individual cages over 24 hours. Locomotor activity (A) and EE (B) measured at baseline of ND in WT and *Aldh6a1*$^{-/-}$ mice over 24. Averaged RER per hour (C) and total 24h EE (D, E) in mice with ND and HFD. The assessment of activity (F, G) during light and dark phase in mice fed ND and HFD. ND: n = 9/9, HFD: n = 10/10, *p <0.01, ***p <0.001. Data are presented as mean ± SEM. Statistical testing, two-tailed unpaired

Student's t test (A, D-G); Mann-Whitney test (B); Two-way ANOVA with multiple comparisons (C).

3.4 No impact of HFD on glucose or insulin tolerance in *Aldh6a1*$^{-/-}$ mice

Next, we examined whether *Aldh6a1* deficiency affected glycemic control and insulin sensitivity. To evaluate this, we obtained monthly plasma samples of non-fasted mice during the intervention and performed an ipGTT as well as an ipITT at the end. Feeding glucose without apparent difference was found between WT and *Aldh6a1*$^{-/-}$ mice regardless of dietary intervention (Fig. 8A, B). However, both ND and HFD-fed *Aldh6a1*$^{-/-}$ mice had lower fasting glucose compared with WT mice at fasting 1h (ND: $p = 0.013$, Fig. 8C, HFD: $p = 0.02$, Fig. 8D), consisting of fasting 3h with HFD feeding ($p = 0.015$, Fig. 8D), but with no difference if fasting 3h between WT and *Aldh6a1*$^{-/-}$ mice fed the ND (Fig. 8C). Glucose curves of ND and HFD groups were similar as ND groups received 2 g/kg glucose bolus, whereas HFD mice were injected 1 g/kg glucose. We did not observe a significant difference between genotypes during the HFD (Fig. 8F); however, glucose tolerance had a minor improvement in *Aldh6a1*$^{-/-}$ fed a ND at only the 15min time point ($p = 0.02$, Fig. 8E). Insulin sensitivity remained similar for WT and *Aldh6a1*$^{-/-}$ mice (Fig. 8G, H). Neither WT nor *Aldh6a1*$^{-/-}$ mice showed a strong impairment of glucose or insulin handling. HFD feeding elevated the insulin level ($F (1, 35) = 11.71$, d=1.613, Fig 8I) and decreased plasma NEFA ($F (1, 36) = 35.13$, $d = 2.794$, Fig. 8J) in WT and *Aldh6a1*$^{-/-}$ mice relative to baseline, showing the anti-lipolytic effect of insulin, albeit without obvious differences between genotypes.

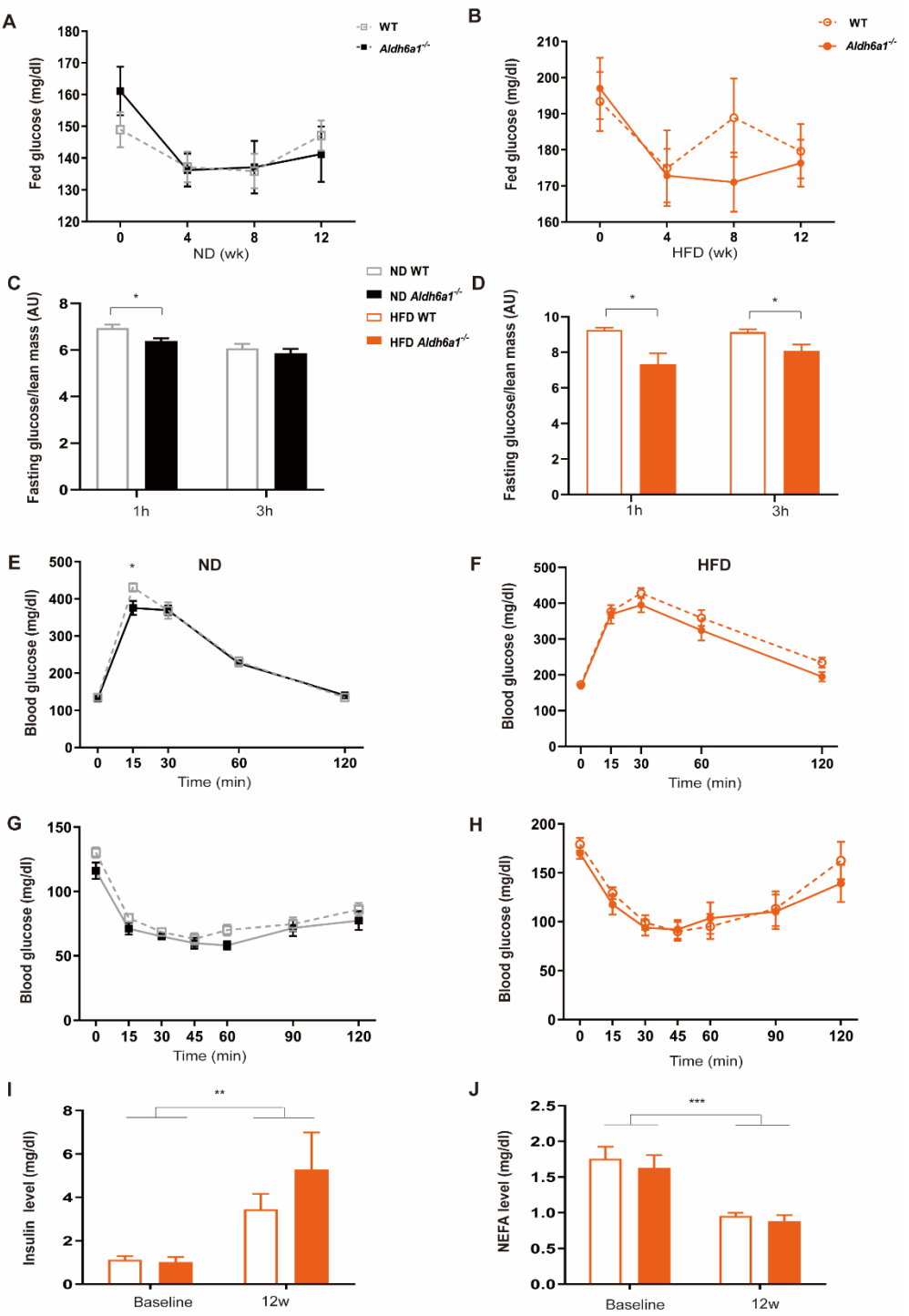

Figure 8 The parameters of glycemic control and NEFA, insulin levels in *Aldh6a1*$^{-/-}$ and WT mice. Fed glucose (A, B) and fasting blood glucose at 1h and 3h (C, D) in mice with ND and HFD for 12 weeks normalized by lean mass. GTT (E, F) and ITT (G, H) were performed in *Aldh6a1*$^{-/-}$ and WT mice fed with ND and HFD intervention. Insulin concentration (I) and NEFA (J) in serum shown at the baseline (0 week) and 12 weeks of HFD intervention. $^{*}p<0.05$, $^{**}p<0.01$ and $^{***}p<0.001$. Values are presented as mean ± SEM. ND: n=10/9, HFD: n=10/10. Statistical testing, two-tailed unpaired Student's t test (A-H); Two-way ANOVA with multiple comparisons (I, J). GTT: intraperitoneal glucose tolerance test, ITT: Insulin tolerance test.

3.5 Mitochondrial respiration and oxidative phosphorylation of *Aldh6a1*-deficient mice feeding HFD

As MMSDH is possibly involved in mitochondrial processes, *Aldh6a1* being involved mostly in oxidative phosphorylation pathway has been reported[76]. We investigated its impact on mitochondrial respiration in various tissues to explore whether *Aldh6a1* is associated with oxidative phosphorylation. To measure mitochondrial respiration and key mitochondrial complexes, we performed seahorse and Western blot analysis with samples of HFD-fed WT and *Aldh6a1*$^{-/-}$mice. After 12 weeks, the oxygen consumption rate (OCR) in freshly isolated biopsies from BAT was similar between *Aldh6a1*$^{-/-}$ and WT mice (The data is not shown in my thesis). Interestingly, we discovered a higher maximal OCR in liver biopsies ($p = 0.04$, Fig. 9A, C). This resulted in an increase of spare capacity (SC) ($p = 0.06$, Fig. 9C), which indicates an improved ability of *Aldh6a1*$^{-/-}$ deficient liver to respond to an increased energy demand during DIO. However, OXPHOS protein did not alter in genotype after HFD feeding (Fig. 9E, G). A similar trend was found in the mitochondrial respiration of eWAT biopsies, but missing significance. (Basal OCR: $p = 0.07$, maximal OCR: $p = 0.08$, Fig. 9B, D). Consistently, OXPHOS complex IV was significantly elevated in *Aldh6a1*$^{-/-}$ mice, which is the most relevant protein for oxidative respiration in mitochondrial ($p = 0.04$, Fig. 9F, H). In addition, no difference was observed in the mitochondrial respiration of liver and eWAT in mice with ND (Fig. 9L, K).

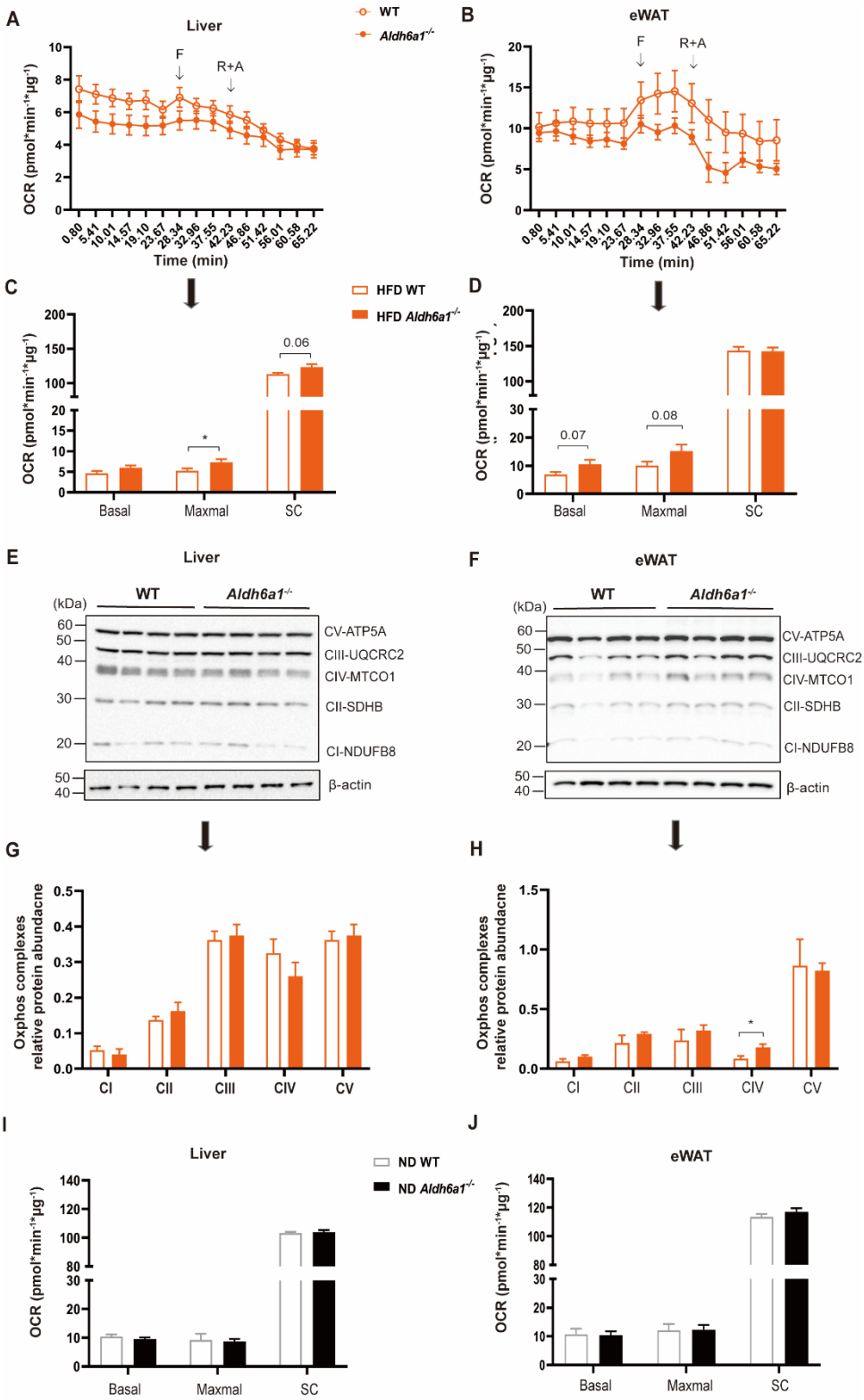

Figure 9 The mitochondrial respiration and oxidative phosphorylation (OXPHOS) complexes I-V of *Aldh6a1*$^{-/-}$ mice in liver and eWAT with HFD and ND. The curve and caculation of the oxygen consumption rate (OCR) in liver (A, C) and eWAT (B, D) of mice fed the HFD (HFD: n = 9/10). Representative Western blots of OXPHOS complexes in liver (E), eWAT (F) in WT and *Aldh6a1*$^{-/-}$ mice with HFD feeding. The corresponding quantification of OXPHOS proteins was calculated

relative to β-actin in liver (G) and eWAT (H). n = 4/4. The basal, maximal OCR and spare capacity (SC) of liver (I) and eWAT (J) in WT and *Aldh6a1*$^{-/-}$ mice with ND is shown. ND: Liver and eWAT (n = 10/9). *p <0.05. Values are presented as mean ± SEM. Statistical testing, two-tailed unpaired Student's t test (A-J). OCR: Oxygen consumption respiration, F: Fluoro-carbonyl cyanide pheylhydrazone, R: Rotenone, A: Antimycin. CI: ATP5A, CII: SDHB, CIII: UQCRC2, CIV: MTCO1, CV: NDUFB8.

3.6 Modulation of lipid, glucose and BCAA parameters in HFD-fed *Aldh6a1*$^{-/-}$ mice

Hypothesizing an *Aldh6a1*$^{-/-}$ deficiency would downregulate BCAA metabolism by blocking valine catabolism, we wondered whether lipid or glucose metabolism would compensate or bypass such a BCAA breakdown defect. Hence, we investigated lipid accumulation and measured transcriptomic regulation of metabolic-relevant genes in this pathway within liver, adipose and skeletal muscle tissue. We observed large but similar storage of ectopic hepatic lipids in liver section for both genotypes (Fig. 10A, B). Triglyceride levels also did not differ in plasma (Fig. 10C), but in liver there may have been a reduction in *Aldh6a1*$^{-/-}$ (Fig. 10D); however, this missed statistical significance. We also did not find a major regulation of relevant genes, rather only slight tendencies for single genes (Fig. 10E).

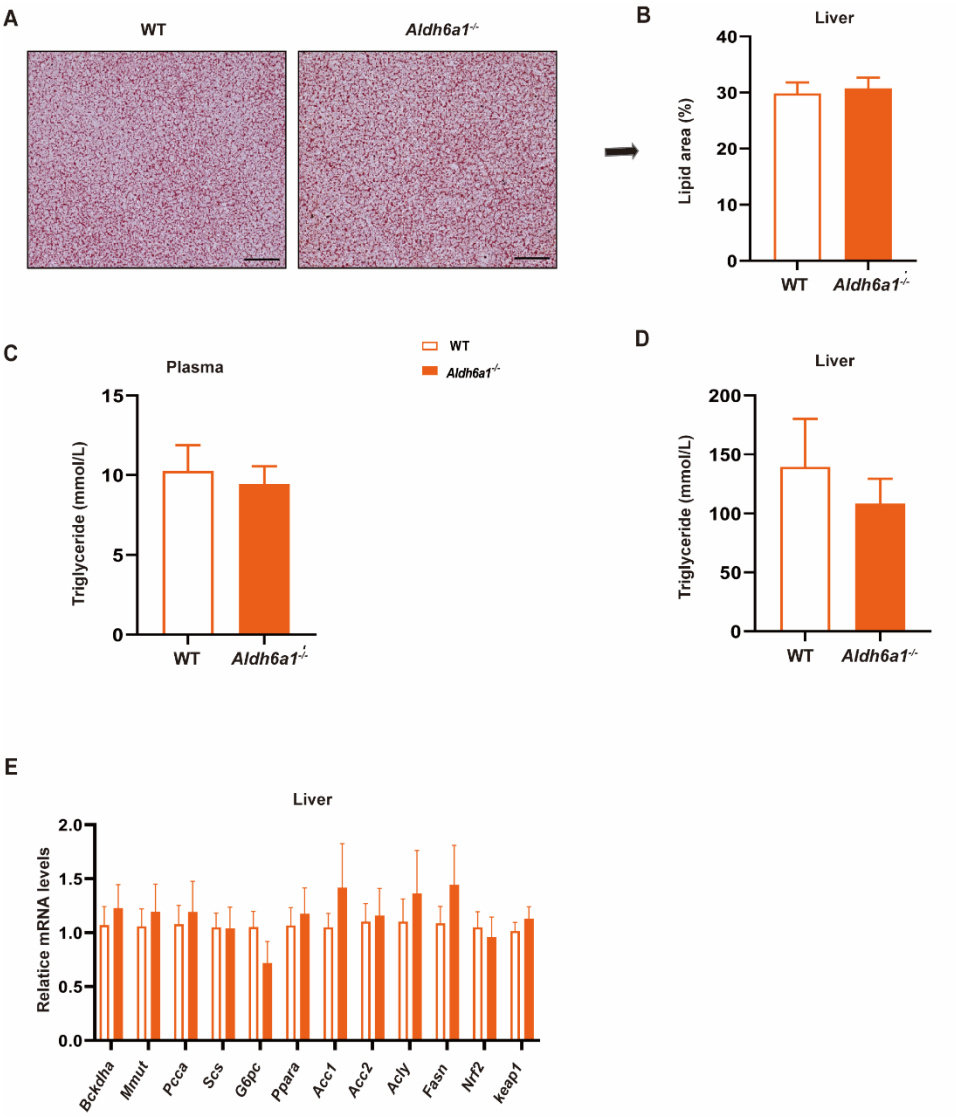

Figure 10 The hepatic lipid metabolism and related genes in HFD-induced mice. Representative images of Oil-Red O staining sections of liver (A) in WT and Aldh6a1-/- mice fed HFD. Images were taken on a 20x field. Average lipid area was evaluated in liver (B). Triglyceride content in plasma (C) and liver (D) from two groups is shown, n = 4/4. Quantitative real-time PCR analysis of genes involved in BCAA, glucose, and lipid metabolism in liver (E), n = 6/6. All data are presented as mean ± SEM. Statistical testing, two-tailed unpaired Student's t-test (B-E).

Interestingly, insulin receptor substrate 1 (IRS1), an enzyme participating in the insulin signaling pathway, was significantly downregulated in eWAT (p=0.02, Fig. 11A) of *Aldh6a1*$^{-/-}$ mice under DIO. Therefore, we examined whether this IRS-1 difference may impact on insulin sensitivity in primary adipocytes from *Aldh6a1*$^{-/-}$ mice stimulated/challenged by glucose or insulin *ex vivo*. However, phosphorylation of AKT (Fig. 11B, C) in the insulin signaling pathway was similar, and the same as glucose uptake (Fig. 11D) between genotypes, and also analyzing lipolytic response showed analog NEFA release (Fig. 11E).

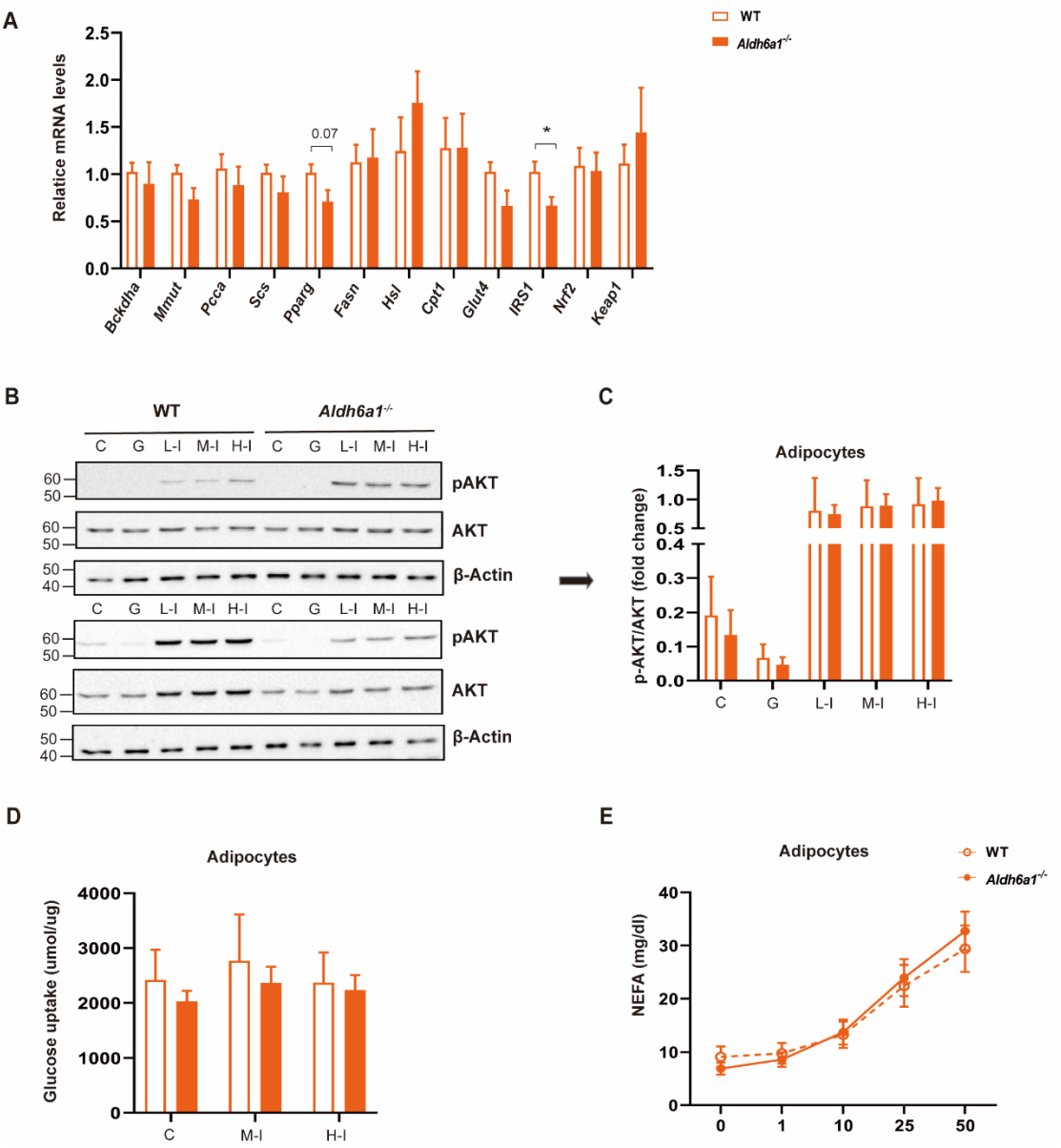

Figure 11 The alterations of the relevant genes in adipose tissue and muscle from WT and *Aldh6a1*$^{-/-}$ mice after HFD feeding. Quantitative real-time PCR analysis of eWAT in HFD-induced obese mice (A), n = 6/6. Western blot analysis of glucose (4.5 g/L, *ex vivo*), insulin (L-I:

10 nM, M-I: 100 nM, H-I: 1000 nM, *ex vivo*) stimulated pAKT and total AKT in adipocytes from WT and KO mice on the HFD with 6% sucrose (B), with densitometric quantification of them on the left side (C), n = 4/4. (D) *Ex vivo* uptake of 2-deoxy-glucose in adipocytes from 12-week mice on the WD, n = 4/4. (E) Isoprenaline-stimulated non-esterified fatty acid (NEFA) analysis in *ex vivo* adipocytes from 12-week mice on the HFD. n = 6/6, *p <0.05. Values are presented as mean ± SEM. Statistical testing, two-tailed unpaired Student's t-test (A-E).

As skeletal muscle is a crucial peripheral tissue for maintaining glucose homeostasis, which usually extracts 1/3 of glucose loading[85], we analyzed qPCR, muscle OCR measurements and insulin signaling *ex vivo* in muscle. However, muscle of *Aldh6a1*$^{-/}$ mice showed a decreased expression of genes involved in BCAA catabolism (*Bckdha*, p = 0.03, *Bcat*, p = 0.03, Fig. 12A) and glucose transport (*Glut* 4, p= 0.01, Fig. 12A). Glut 4 is insulin-regulated glucose transporter in muscle. Thus, we next performed insulin signaling in SOL by stimulation with insulin and Nacl *ex vivo* to detect the insulin sensitivity of muscle. But no difference in pAKT abundance (Fig. 12B, C) of SOL was observed between WT and *Aldh6a1*$^{-/}$ mice with the HFD. Interestingly, there was down-regulation of succinyl-CoA synthetase (*Scs*, p = 0.01, Fig. 12A), an enzyme of succinate synthesis, in *Aldh6a1*$^{-/}$ mice relative to the WT group during the HFD. Given that succinates are the substrates of the TCA cycle, we further identified whether it affects mitochondrial oxidative, and both WT and *Aldh6a1*$^{-/}$ mice showed a similar tendency of mitochondrial respiration in muscle (Fig. 12D, E)

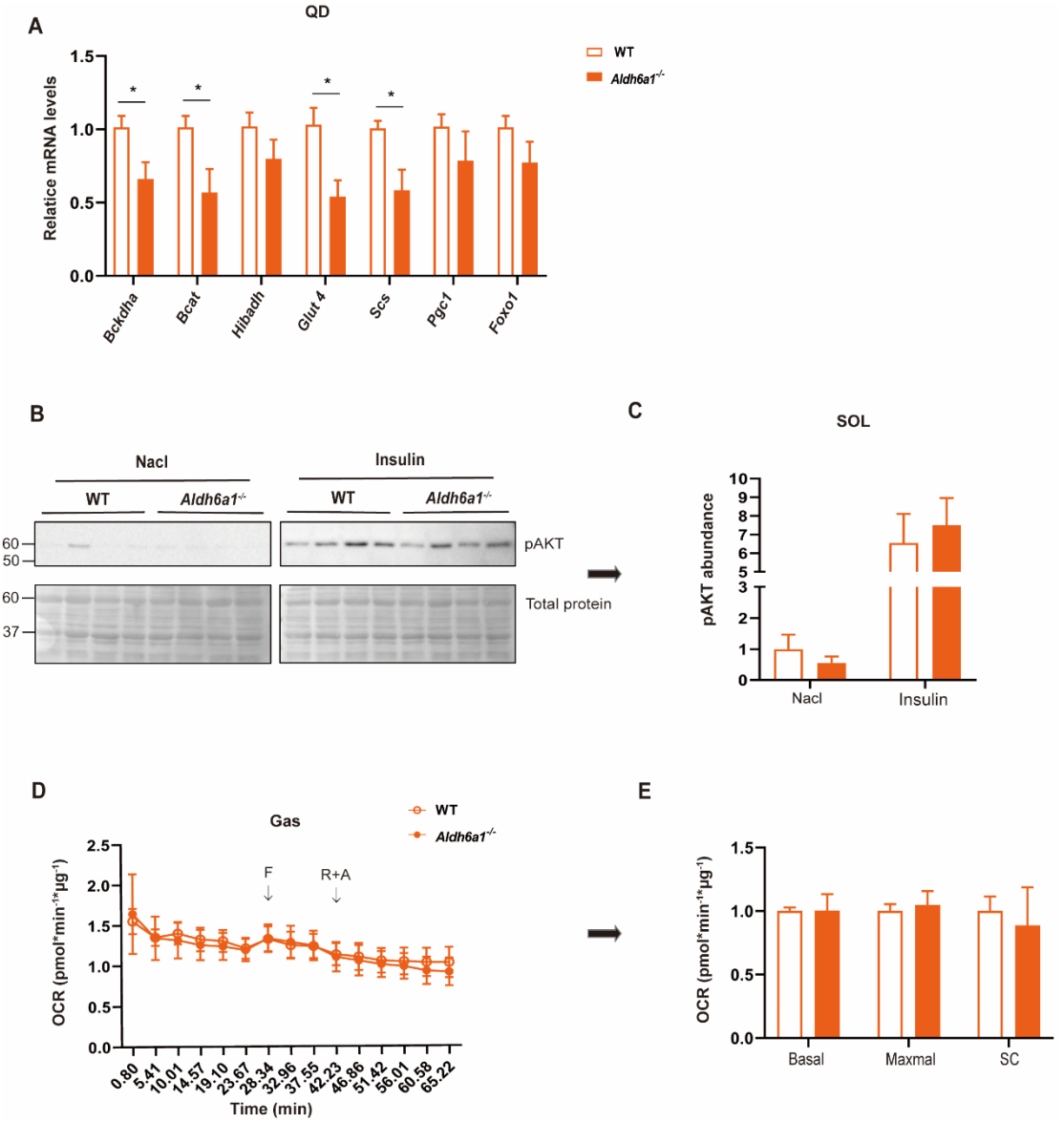

Figure 12 The regulation of genes in muscle from WT and *Aldh6a1*$^{-/-}$ mice after HFD feeding. Quantitative real-time PCR analysis from QD in HFD-induced obese mice (A), n = 6/6. Western blot analysis of phosphorylation AKT (pAKT) and total protein of SOL stimulated by Nacl (0.9%, *ex vivo*), insulin (100 nM, ex vivo) in mice (B), and densitometric quantification of them both (C), n = 4/4. The mitochondrial respiration (D) and the corresponding calculation of OCR (E) in Gas are shown, n = 4/4. *p <0.05. Values are presented as mean ± SEM. Statistical testing, two-tailed unpaired Student's t-test (A, C, E).

4. Discussion

This work investigates the metabolic role of the *Aldh6a1*-deficient mouse model during DIO and its molecular function. Previous research described *ALDH6A1* as a new marker of muscle IR and its possible involvement in adipose tissue-related oxidative phosphorylation in obese patients with T2D[75-77,80,86]. Therefore, we supposed that *Aldh6a1*$^{-/-}$ mice would aggravate DIO and affect the mitochondrial oxidative during HFD intervention. In contrast, our study revealed that *Aldh6a1*$^{-/-}$ mice slightly resist DIO by increasing lean mass, in line with enhanced diet and water consumption as well as improved fasting glucose. Our results analyzing mitochondrial respiration further showed that *Aldh6a1*$^{-/-}$ mice had elevated liver mitochondrial respiration if there was high-energy demand. A slightly increased mitochondrial respiration in eWAT was observed by trend, together with increased abundance of mitochondrial complex IV in HFD-fed *Aldh6a1*$^{-/-}$ mice. However, we did not observe an effect of *Aldh6a1* ablation in GTT or ITT, but a downregulation of genes related to glucose transport in skeletal muscle (quadriceps). These results suggest that ALDH6A1 slightly improves the metabolic profile during DIO. Further investigations are warranted to elucidate the potential mechanism underlying this phenotype.

4.1 Tissue expression and validation of *Aldh6a1* deficiency

Our work employed an *Aldh6a1*-deficient mouse line, in which the murine *Aldh6a1* was targeted in all tissues by CRISPR-Cas9, resulting in an 11 bp deletion within exon 2 of the *Aldh6a1* gene. *Aldh6a1*$^{-/-}$ mice have a slight residual expression of *Aldh6a1* mRNA in qPCR, which is absent at the protein level, presumably because of transcribed but not translated pre-mRNA. Since *Aldh6a1* encodes the enzyme MMSDH, the protein is essential for its function and we consider our mouse model as successful and ALDH6A1/MMSDH as dysfunctional. We found a high abundance of ALDH6A1 in heart, liver, muscle, kidney, BAT and adipose tissue of male WT mice. A previous study showed a different pattern of expression and abundance rank in rat tissues, perhaps due to species difference[63]. We used only male mice to study metabolic profiles due to estrogen effects in females[84] and male-dominant cases in the clinic. We did not observe any abnormal (body) development, signs of motor deficit or weight loss in *Aldh6a1*$^{-/-}$ mice. Therefore, homozygous *Aldh6a1* deletion is not lethal and its deficiency seems to

be circumvented or covered in our mouse model. For human patients with *ALDH6A1* mutation, heterogeneous clinical manifestations are described including weight loss, severe developmental delays or hypotonia[65,66,68]. Besides those clinical manifestations, some patients have gastroesophageal reflux or diarrhea dehydration, which indicates heterogeneity of clinical symptoms in patients.

4.2 The effects of *Aldh6a1* ablation on HFD-induced obesity

To study the impact of whole-body *Aldh6a1* deficiency, we analyzed *Aldh6a1*$^{-/-}$ and WT mice during the ND, and also challenged the with the HFD to characterize metabolic parameters such as body composition, daily food and drink consumption. Both genotypes gained weight during 12 weeks of ND and HFD feeding. A slightly increased body weight, as well as lean mass, were found in *Aldh6a1*$^{-/-}$ mice under the ND by trend, while fat mass gain was slightly decreased.

During the HFD Aldh6a1$^{-/-}$ mice showed that they had gained more lean mass - however, without a significant difference in fat mass- and, interestingly, the body weight was only slightly higher but not statistically different. Lean, i.e., fat-free mass, which mainly consists of muscles and organs, is considered as a predictor of mortality, that is better than BMI[87]. Usually, HFD feeding decreases food and water intake in mice compared to the ND. This lower HFD intake is probably driven by a feedback loop of satiety signals, whereby over-nutrition elevates circulatory fuel substrates, such as glucose and fatty acids, to stimulate brain nutrient-sensing systems[88]. Previous studies have shown that rats fed an HFD had lower water intake than standard chow-fed rats[89-91]. Interestingly, *Aldh6a1*$^{-/-}$ mice during DIO exhibited increased diet intake, presumably caused by valine-deficient supply, resulting in increased demand of leucine and isoleucine. Since leucine and isoleucine may replace the function of valine catabolism, such as for propionyl-Co A production, this might lead to more water consumption immediately after eating food to reduce the osmotic and volumetric stimulation of thirst[92]. Increased water and food intake affect body composition, which is consistent with increased lean mass in *Aldh6a1*$^{-/-}$ mice fed on the HFD. Notably, *Aldh6a1*$^{-/-}$ mice gain more lean mass with a slightly decreased tendency of fat gain, whereas the literature describes that 3-4 weeks of HFD feeding are sufficient to increase fat mass, leading to obesity[86]. *Aldh6a1*$^{-/-}$ mice may have maintained better hydration to resist obesity due to increased lean mass. A previous study found a 30% increase in the metabolic rate 30-40 min after drinking 500

ml water in both men and women[93]. In addition, increased water intake may lower the vasopressin level and improve the metabolic profile[94]. Obese rats with low vasopressin levels have been demonstrated to have improved liver steatosis and reduced hepatic lipogenesis[95]. Furthermore, another possibility is that increased food intake caused by isoleucine and leucine compensation would contribute to lean mass gain, as it has been reported that isoleucine is critical in regulating body weight, leading to muscle protein synthesis[96]. Similarly, 80% of leucine is used for protein synthesis, and leucine and its metabolites (HMB hydroxyl-beta-methylbutyrate, α-KIC α-ketoisocaproate) in protein synthesis contribute to increased lean body mass[97].

The mechanism behind this could be increased food intake caused by isoleucine and leucine compensation leading to take more water intake, which leads to a gaining of lean mass by improving hydration and lipid mobilization under DIO. Sympathetic activation and stimulation of β-adrenergic receptors or body hydration may be responsible. Overall, the increased diet intake combined with elevated water consumption of Aldh6a1$^{-/-}$ mice during the HFD may be the reason for the pronounced lean mass increase instead of fat accumulation, without affecting total body weight.

4.3 Energy balance in Aldh6a1$^{-/-}$ mice fed an HFD

Energy balance consists of energy intake, energy expenditure and energy storage and is in a positive state during obesity. Diet consists of protein, fat and carbohydrates, and energy output is classified as EE, food-induced thermogenesis and physical activity[98]. In our study, no difference of EE and physical activity was obvious in *Aldh6a1*$^{-/-}$ mice at baseline. However, after 12 weeks of ND, *Aldh6a1*$^{-/-}$ mice exhibited an increased EE that just missed significance. Consistently, increased total EE has been reported in isoleucine, valine or leucine-deprived mice[99]. Furthermore, research showed that C57BL/6J mice fed a diet low in AA, specifically in BCAA, had increased RER and EE, and restoration of valine alone had only minimal effects on these parameters[54]. Since an enhanced EE without hyperphagia was observed in rats with a protein-restricted diet[100], it may be supposed that increased EE is the first response to a low BCAA diet by blocking valine metabolism. However, *Aldh6a1*$^{-/-}$ mice during the HFD showed no difference in EE, while inconsistently, a WD (HFD+6% sucrose) with low BCAA promoted EE in mice[53]. This may imply that excess glucose needs to be consumed through EE to resist obesity under the WD. Due to the increased HFD intake and unchanged EE,

Aldh6a1$^{-/-}$ mice exhibited a positive energy balance, which may be required for the elevated lean mass gain, in line with the increased lean mass gain in our *Aldh6a1*$^{-/-}$ mice. Activity did not differ between genotypes under the ND and HFD. This is in line with the unchanged physical activity of mice fed a low valine diet[99].

In conclusion, we only found slightly increased EE in *Aldh6a1*$^{-/-}$ mice with ND, but no difference in EE during the HFD. A negative feedback mechanism compensating the *Aldh6a1* deficiency cannot be excluded as, e.g., an upregulation of leucine and isoleucine caused by valine deficiency may neutralize increased EE due to the blocking of valine. There is evidence of isoleucine and leucine-restricted diets as well as valine deprivation to increasing EE in mice[101,102]. Further investigations are warranted to examine the BCAA metabolism in *Aldh6a1*$^{-/-}$ mice.

4.4 HFD-fed *Aldh6a1*$^{-/-}$ mice showed improved fasting glucose

Next, we studied glucose and insulin tolerance to evaluate glucose homeostasis and insulin sensitivity in HFD-fed *Aldh6a1*$^{-/-}$ mice. First, we revealed lower fasting glucose levels of ND-fed *Aldh6a1*$^{-/-}$ mice after short-term fasting of 1 h, but not 3 h. Notably, this was accompanied by an improved peak glucose after 15 min of the ipGTT, whereas insulin tolerance remained unchanged. Therefore, glucose homeostasis seems mildly affected by the genotype, which is in agreement with Yu *et al*., showing mice fed a low valine diet had a trend toward improved glucose tolerance ($p = 0.06$) along with normal insulin tolerance[54]. Since ALDH6A1 is associated positively with fasting IS[109], we hypothesize that *Aldh6a1*$^{-/-}$mice may exhibit IR and worse glucose control under DIO. In contrast, HFD-fed *Aldh6a1*$^{-/-}$ mice showed lower blood glucose at 1 h and 3 h of fasting after being normalized by lean mass, but no differences in glucose or insulin tolerance compared with WT mice during DIO. These results indicate that downregulation of ALDH6A1 is the consequence of IR in T2D, but *Aldh6a1* deficiency is not causative for IR. Consistently, previous research showed decreased fasting blood glucose and insulin in mice fed a WD with low BCAA[53]. It is implied that more glucose supplies hepatic and muscle glycogen production in *Aldh6a1*$^{-/-}$ mice due to valine deficiency (glycogenic amino acid). Thus, *Aldh6a1*$^{-/-}$ mice had improved fasting glucose when either fed ND or HFD. We suppose that the *Aldh6a1* knockout mimics low BCAA diets and, therefore, may contribute to improve fasting glucose.

4.5 The improved oxidative phosphorylation in liver and adipose tissue in *Aldh6a1*$^{-/-}$ mice fed an HFD

In 2020, a case report of ALDH6A1 mutation showed reduced oxygen with increased superoxide production in patient fibroblasts[68]. However, we did not observe alterations of mitochondrial respiration and complexes in muscle. This is in line with another case report of ALDH6A1 mutation, in which no changes of the respiratory chain were observed in frozen muscle and skin fibroblasts by electron microscopy[103]. Interestingly, we observed an increased ability of *Aldh6a1*$^{-/-}$ liver to respond to higher energy demand. We assume that blocking valine catabolism decreases the 3HIBA level, which could be one reason for improved mitochondrial oxidative in liver. The previous study indicated that high circulating 3-HIBA reflect reduced fatty acid oxidation, and therapies of lowering 3HIBA may increase fatty acid oxidation in liver[104]. Our results may reflect that *Aldh6a1*$^{-/-}$ mice increased the capacity of hepatic mitochondrial oxidative during DIO due to the lowering of 3-HIBA by valine deficiency. A dysregulated oxidative phosphorylation pathway was found in both obese adipose tissue and atherosclerotic plaques, while *Aldh6a1* has been identified as a high-ranking gene related to oxidative phosphorylation[76]. In contrast, we discovered an enhanced abundance of OXPHOS complex IV with a slightly increased mitochondrial respiration in the eWAT of *Aldh6a1*$^{-/-}$ mice fed an HFD. Consistently, 3HIBA is a potentially important regulator of adipocyte mitochondrial respiration, and adipocytes decreased maximal mitochondrial respiration if 3HIBA was added[105]. Thus, lowering 3HIBA may contribute to improved mitochondrial respiration of WAT by increasing complex IV in *Aldh6a1*$^{-/-}$ mice.

4.6 Regulation of BCAA and glucose catabolic genes in HFD-fed muscle

The liver is an essential organ regulating glucose homeostasis, however we found no impact of aldh6a1 deficiency on hepatic key genes involved in glycolysis, lipid synthesis, lipolysis and BCAA catabolism during HFD. Beyond this, we identified a downregulation of *Irs1* in eWAT and *Glut4* in muscle in *Aldh6a1*$^{-/-}$ mice during the HFD. DIO induces IR in peripheral tissue (such as adipose tissue and muscle) due to a chronic inflammatory state. However, our *ex vivo* assessment of insulin signaling did not reveal differences in glucose transport and insulin sensitivity, although previous studies reported a positive correlation of ALDH6A1 with fasting IR in the muscle of patients with metabolism disease[106] along with a decreased *ALDH6A1* expression as a new marker of muscle IR in

T2DM patients[80]. We assume a compensatory mechanism circumventing the *Aldh6a1*/MMSDH deficiency may decrease intermediates of the blocked valine catabolism (3HIBA, AIBA) in *Aldh6a1*$^{-/-}$ mice. Lower 3HIBA could counteract the supposed advantages of lower AIBA due to their opposing effects in the IR of peripheral tissues. 3HIBA is positively related to adipose IR in T2DM and obesity[69] and promotes FFA transport by endothelial cells, thereby increasing muscle lipid content and amplifying IR in mice[55]. AIBA, on the other hand, not only improves IR and inflammation in muscle after exercise[107,108], but also enhances EE by increasing fatty acids β-oxidation[71].

In summary, downregulation of genes related to BCAA catabolism and glucose transport were found in muscle but did not alter the insulin signaling in *Aldh6a1*$^{-/-}$ mice during the HFD. Therefore, future experiments are necessary to evaluate the regulation of valine, leucine, isoleucine and their intermediates 3HIBA, AIBA in *Aldh6a1*$^{-/-}$ mice to elucidate their specific metabolic role.

5. Conclusions

In conclusion, we showed a comprehensive metabolic analysis of a novel *Aldh6a1*-deficient mouse model. *Aldh6a1* deficiency slightly attenuated diet-induced obesity in male mice with increased lean mass gain and improved fasting glucose, accompanied by downregulation of insulin signaling genes transcriptionally without IR in peripheral tissues. Additionally, we indicated an enhanced hepatic mitochondrial flexibility and a better mitochondrial oxidative of adipose tissue in *Aldh6a1*$^{-/-}$ mice with DIO. We demonstrated that *Aldh6a1* is not the key for insulin sensitivity or oxidative phosphorylation pathway. Furthermore, our study contributes to recognition of the function of ALDH6A1.

6. Limitation

Our study did not investigate female *Aldh6a1*$^{-/-}$ mice for the reported changes, since we considered that female mice may exhibit different phenotypes due to estrogen effects. Moreover, the *Aldh6a1*$^{-/-}$ mouse line was a whole-body knockout, so might specific *Aldh6a1*$^{-/-}$ in muscle of mice could have different phenotype. Further experiments are necessary to evaluate metabolites of valine catabolism and AA Profile to elucidate their specific compensatory mechanism.

References

1. Organization WH. World Health Organization.Obesity : preventing and managing the global epidemic : report of a WHO consultation. Geneva: World Health Organization; 2000.
2. World Health Organization, "Obesity". Octorber 2021: https://www.who.int/health-topics/obesity.
3. Trends in adult body-mass index in 200 countries from 1975 to 2014: a pooled analysis of 1698 population-based measurement studies with 19·2 million participants. *The Lancet* 2016; **387**(10026): 1377-96.
4. Chen K, Xie Y, Hu P, Zhao S, Mo Z. Multiple Symmetric Lipomatosis: Substantial Subcutaneous Adipose Tissue Accumulation Did Not Induce Glucose and Lipid Metabolism Dysfunction. *Annals of Nutrition and Metabolism* 2010; **57**(1): 68-73.
5. Messier V, Karelis AD, Prud'homme D, Primeau V, Brochu M, Rabasa-Lhoret R. Identifying Metabolically Healthy but Obese Individuals in Sedentary Postmenopausal Women. *Obesity* 2010; **18**(5): 911-7.
6. Meisinger C DA, Thorand B, Heier M, Lowel H. Body fat distribution and risk of type 2 diabetes in the general population are there differences between men and women The MONICAKORA Augsburg cohort study. *Am J Clin Nutr* 2006; **84**: 483-9.
7. S.R F. Transcriptional control of adipocyte formation. *Cell Metab* 2006; **4**(4): 263-73.
8. Lackey DE, Olefsky JM. Regulation of metabolism by the innate immune system. *Nature Reviews Endocrinology* 2015; **12**(1): 15-28.
9. Galletti F, Barbato A Fau - Versiero M, Versiero M Fau - Iacone R, Iacone R Fau - Russo O, Russo O Fau - Barba G, Barba G Fau - Siani A, Siani A Fau - Cappuccio FP, Cappuccio Fp Fau - Farinaro E, Farinaro E Fau - della Valle E, della Valle E Fau - Strazzullo P, Strazzullo P. Circulating leptin levels predict the development of metabolic syndrome in middle-aged men: an 8-year follow-up study. *J Hypertnes* 2007; **25**(8): 1671-7.
10. Kusminski CM, Scherer PE. Leptin Beyond the Lipostat Key Component of Blood Pressure Regulation. *Circ Res* 2015; **116**(8): 1293-5.
11. Yamauchi T, Kamon J, Waki H, Imai Y, Shimozawa N, Hioki K, Uchida S, Ito Y, Takakuwa K, Matsui J, Takata M, Eto K, Terauchi Y, Komeda K, Tsunoda M, Murakami K, Ohnishi Y, Naitoh T, Yamamura K, Ueyama Y, Froguel P, Kimura S, Nagai R,

Kadowaki T. Globular adiponectin protected ob/ob mice from diabetes and ApoE-deficient mice from atherosclerosis. *J Biol Chem* 2003; **278**(4): 2461-8.

12. Ye R, Scherer PE. Adiponectin, driver or passenger on the road to insulin sensitivity? *Mol Metab* 2013; **2**(3): 133-41.

13. Wernstedt Asterholm I, Tao C, Morley TS, Wang QA, Delgado-Lopez F, Wang ZV, Scherer PE. Adipocyte inflammation is essential for healthy adipose tissue expansion and remodeling. *Cell Metab* 2014; **20**(1): 103-18.

14. Gastaldelli A. Role of beta-cell dysfunction, ectopic fat accumulation and insulin resistance in the pathogenesis of type 2 diabetes mellitus. *Diabetes Res Clin Pr* 2011; **93**: S60-S5.

15. Ismail-Beigi F. Pathogenesis and Glycemic Management of Type 2 Diabetes Mellitus: A Physiological Approach. *Arch Iran Med* 2012; **15**(4): 239-46.

16. Roglic G, Unwin N. Mortality attributable to diabetes: Estimates for the year 2010. *Diabetes Res Clin Pr* 2010; **87**(1): 15-9.

17. Cho NH, Shaw JE, Karuranga S, Huang Y, Fernandes JDD, Ohlrogge AW, Malanda B. IDF Diabetes Atlas: Global estimates of diabetes prevalence for 2017 and projections for 2045. *Diabetes Res Clin Pr* 2018; **138**: 271-81.

18. Holman N, Young B, Gadsby R. Current prevalence of Type 1 and Type 2 diabetes in adults and children in the UK. *Diabetic Med* 2015; **32**(9): 1119-20.

19. Diamond J. MEDICINE Diabetes in India. *Nature* 2011; **469**(7331): 478-9.

20. Yang WY, Lu JM, Weng JP, Jia WP, Ji LN, Xiao JZ, Shan ZY, Liu J, Tian HM, Ji QH, Zhu DL, Ge JP, Lin LX, Chen L, Guo XH, Zhao ZG, Li Q, Zhou ZG, Shan GL, He J, Disorders CNDM. Prevalence of Diabetes among Men and Women in China. *New Engl J Med* 2010; **362**(12): 1090-101.

21. Weigensberg MJ, Goran MI. Type 2 diabetes in children and adolescents. *Lancet* 2009; **373**(9677): 1743-4.

22. Frayling TM, Timpson NJ, Weedon MN, Zeggini E, Freathy RM, Lindgren CM, Perry JRB, Elliott KS, Lango H, Rayner NW, Shields B, Harries LW, Barrett JC, Ellard S, Groves CJ, Knight B, Patch AM, Ness AR, Ebrahim S, Lawlor DA, Ring SM, Ben-Shlomo Y, Jarvelin MR, Sovio U, Bennett AJ, Melzer D, Ferrucci L, Loos RJF, Barroso I, Wareham NJ, Karpe F, Owen KR, Cardon LR, Walker M, Hitman GA, Palmer CNA, Doney ASF, Morris AD, Smith GD, Hattersley AT, McCarthy MI, Control WTC. A common variant in the FTO gene is associated with body mass index and predisposes to childhood and adult obesity. *Science* 2007; **316**(5826): 889-94.

23. Saxena R, Voight BF, Lyssenko V, Burtt NP, de Bakker PIW, Chen H, Roix JJ, Kathiresan S, Hirschhorn JN, Daly MJ, Hughes TE, Groop L, Altshuler D, Almgren P, Florez JC, Meyer J, Ardlie K, Bostrom KB, Isomaa B, Lettre G, Lindblad U, Lyon HN, Melander O, Newton-Cheh C, Nilsson P, Orho-Melander M, Rastam L, Speliotes EK, Taskinen MR, Tuomi T, Guiducci C, Berglund A, Carlson J, Gianniny L, Hackett R, Hall L, Holmkvist J, Laurila E, Sjogren M, Sterner M, Surti A, Svensson M, Svensson M, Tewhey R, Blumenstiel B, Parkin M, DeFelice M, Barry R, Brodeur W, Camarata J, Chia N, Fava M, Gibbons J, Handsaker B, Healy C, Nguyen K, Gates C, Sougnez C, Gage D, Nizzari M, Gabriel SB, Chirn GW, Ma QC, Parikh H, Richardson D, Ricke D, Purcell S, In DGIB, Res NIB. Genome-wide association analysis identifies loci for type 2 diabetes and triglyceride levels. *Science* 2007; **316**(5829): 1331-6.

24. Scott LJ, Mohlke KL, Bonnycastle LL, Willer CJ, Li Y, Duren WL, Erdos MR, Stringham HM, Chines PS, Jackson AU, Prokunina-Olsson L, Ding CJ, Swift AJ, Narisu N, Hu T, Pruim R, Xiao R, Li XY, Conneely KN, Riebow NL, Sprau AG, Tong M, White PP, Hetrick KN, Barnhart MW, Bark CW, Goldstein JL, Watkins L, Xiang F, Saramies J, Buchanan TA, Watanabe RM, Valle TT, Kinnunen L, Abecasis GR, Pugh EW, Doheny KF, Bergman RN, Tuomilehto J, Collins FS, Boehnke M. A genome-wide association study of type 2 diabetes in Finns detects multiple susceptibility variants. *Science* 2007; **316**(5829): 1341-5.

25. Sladek R, Rocheleau G, Rung J, Dina C, Shen L, Serre D, Boutin P, Vincent D, Belisle A, Hadjadj S, Balkau B, Heude B, Charpentier G, Hudson TJ, Montpetit A, Pshezhetsky AV, Prentki M, Posner BI, Balding DJ, Meyre D, Polychronakos C, Froguel P. A genome-wide association study identifies novel risk loci for type 2 diabetes. *Nature* 2007; **445**(7130): 881-5.

26. Steinthorsdottir V, Thorleifsson G, Reynisdottir I, Benediktsson R, Jonsdottir T, Walters GB, Styrkarsdottir U, Gretarsdottir S, Emilsson V, Ghosh S, Baker A, Snorradottir S, Bjarnason H, Ng MCY, Hansen T, Bagger Y, Wilensky RL, Reilly MP, Adeyemo A, Chen YX, Zhou J, Gudnason V, Chen GJ, Huang HX, Lashley K, Doumatey A, So WY, Ma RCY, Andersen G, Borch-Johnsen K, Jorgensen T, van Vliet-Ostaptchouk JV, Hofker MH, Wijmenga C, Christiansen C, Rader DJ, Rotimi C, Gurney M, Chan JCN, Pedersen O, Sigurdsson G, Gulcher JR, Thorsteinsdottir U, Kong A, Stefansson K. A variant in CDKAL1 influences insulin response and risk of type 2 diabetes. *Nat Genet* 2007; **39**(6): 770-5.

27. Wellcome Trust Case Control C. Genome-wide association study of 14,000 cases of seven common diseases and 3,000 shared controls. *Nature* 2007; **447**(7145): 661-78.

28. Zeggini E, Weedon MN, Lindgren CM, Frayling TM, Elliott KS, Lango H, Timpson NJ, Perry JRB, Rayner NW, Freathy RM, Barrett JC, Shields B, Morris AP, Ellard S, Groves CJ, Harries LW, Marchini JL, Owen KR, Knight B, Cardon LR, Walker M, Hitman GA, Morris AD, Doney ASF, McCarthy MI, Hattersley AT, Wtccc. Replication of genome-wide association signals in UK samples reveals risk loci for type 2 diabetes. *Science* 2007; **316**(5829): 1336-41.

29. Grarup N, Sandholt CH, Hansen T, Pedersen O. Genetic susceptibility to type 2 diabetes and obesity: from genome-wide association studies to rare variants and beyond. *Diabetologia* 2014; **57**(8): 1528-41.

30. Jenkinson CP, Goring HH, Arya R, Blangero J, Duggirala R, DeFronzo RA. Transcriptomics in type 2 diabetes: Bridging the gap between genotype and phenotype. *Genom Data* 2016; **8**: 25-36.

31. Schwartz SS, Epstein S, Corkey BE, Grant SFA, Gavin JR, Aguilar RB. The Time Is Right for a New Classification System for Diabetes: Rationale and Implications of the beta-Cell-Centric Classification Schema. *Diabetes Care* 2016; **39**(2): 179-86.

32. Qin J, Li Y, Cai Z, Li S, Zhu J, Zhang F, Liang S, Zhang W, Guan Y, Shen D, Peng Y, Zhang D, Jie Z, Wu W, Qin Y, Xue W, Li J, Han L, Lu D, Wu P, Dai Y, Sun X, Li Z, Tang A, Zhong S, Li X, Chen W, Xu R, Wang M, Feng Q, Gong M, Yu J, Zhang Y, Zhang M, Hansen T, Sanchez G, Raes J, Falony G, Okuda S, Almeida M, LeChatelier E, Renault P, Pons N, Batto JM, Zhang Z, Chen H, Yang R, Zheng W, Li S, Yang H, Wang J, Ehrlich SD, Nielsen R, Pedersen O, Kristiansen K, Wang J. A metagenome-wide association study of gut microbiota in type 2 diabetes. *Nature* 2012; **490**(7418): 55-60.

33. Pittas AG, Sun Q, Manson JE, Dawson-Hughes B, Hu FB. Plasma 25-hydroxyvitamin D concentration and risk of incident type 2 diabetes in women. *Diabetes Care* 2010; **33**(9): 2021-3.

34. Yoshida M, Booth SL, Meigs JB, Saltzman E, Jacques PF. Phylloquinone intake, insulin sensitivity, and glycemic status in men and women. *Am J Clin Nutr* 2008; **88**(1): 210-5.

35. Gabryelska A, Karuga FF, Szmyd B, Białasiewicz P. HIF-1α as a Mediator of Insulin Resistance, T2DM, and Its Complications: Potential Links With Obstructive Sleep Apnea. *Frontiers in Physiology* 2020; **11**.

36. Ioja S, Weir ID, Rennert NJ. Relationship Between Sleep Disorders and the Risk for Developing Type 2 Diabetes Mellitus. *Postgrad Med* 2012; **124**(4): 119-29.

37. Alberti KGMM, Eckel RH, Grundy SM, Zimmet PZ, Cleeman JI, Donato KA, Fruchart JC, James WPT, Loria CM, Smith SC. Harmonizing the Metabolic Syndrome A Joint Interim Statement of the International Diabetes Federation Task Force on Epidemiology and Prevention; National Heart, Lung, and Blood Institute; American Heart Association; World Heart Federation; International Atherosclerosis Society; and International Association for the Study of Obesity. *Circulation* 2009; **120**(16): 1640-5.

38. Moore JX, Chaudhary N, Akinyemiju T. Metabolic Syndrome Prevalence by Race/Ethnicity and Sex in the United States, National Health and Nutrition Examination Survey, 1988–2012. *Preventing Chronic Disease* 2017; **14**.

39. Wang Y, Mi J, Shan XY, Wang QJ, Ge KY. Is China facing an obesity epidemic and the consequences? The trends in obesity and chronic disease in China. *Int J Obes (Lond)* 2007; **31**(1): 177-88.

40. Athyros VG, Tziomalos K, Karagiannis A, Mikhailidis DP. Dyslipidaemia of obesity, metabolic syndrome and type 2 diabetes mellitus: the case for residual risk reduction after statin treatment. *Open Cardiovasc Med J* 2011; **5**: 24-34.

41. GI BGaS. Free fatty acids in obesity and type 2 diabetes defining their role in the development of insulin resistance and β-cell dysfunction. *Eur J Clin Invest* 2002; **32**(Suppl.3): 14-23.

42. Haas JT, Biddinger SB. Dissecting the role of insulin resistance in the metabolic syndrome. *Curr Opin Lipidol* 2009; **20**(3): 206-10.

43. Wisse BE. The inflammatory syndrome: the role of adipose tissue cytokines in metabolic disorders linked to obesity. *J Am Soc Nephrol* 2004; **15**(11): 2792-800.

44. Tsigos C, Kyrou L, Chala E, Tsapogas P, Stavridis JC, Raptis SA, Katsilambros N. Circulating tumor necrosis factor alpha concentrations are higher in abdominal versus peripheral obesity. *Metabolism* 1999; **48**(10): 1332-5.

45. Vaneckova I, Maletinska L, Behuliak M, Nagelova V, Zicha J, Kunes J. Obesity-related hypertension: possible pathophysiological mechanisms. *J Endocrinol* 2014; **223**(3): R63-78.

46. Kabir M, Catalano KJ, Ananthnarayan S, Kim SP, Van Citters GW, Dea MK, Bergman RN. Molecular evidence supporting the portal theory: a causative link between visceral adiposity and hepatic insulin resistance. *Am J Physiol-Endoc M* 2005; **288**(2): E454-E61.

47. Ying W, Fu W, Lee YS, Olefsky JM. The role of macrophages in obesity-associated islet inflammation and beta-cell abnormalities. *Nat Rev Endocrinol* 2020; **16**(2): 81-90.

48. Batch BC, Hyland K Fau - Svetkey LP, Svetkey LP. Branch chain amino acids: biomarkers of health and disease. *Curr Opin Clin Nutr Metab Care* 2014; **17**(1): 86-9.

49. White PJ, Newgard CB. Branched-chain amino acids in disease. *Science* 2019; **363**(6427): 582-3.

50. Shimomura Y, Murakami T, Nakai N, Nagasaki M, Harris RA. Exercise Promotes BCAA Catabolism: Effects of BCAA Supplementation on Skeletal Muscle during Exercise. *The Journal of Nutrition* 2004; **134**(6): 1583S-7S.

51. McCormack SE, Shaham O, McCarthy MA, Deik AA, Wang TJ, Gerszten RE, Clish CB, Mootha VK, Grinspoon SK, Fleischman A. Circulating branched-chain amino acid concentrations are associated with obesity and future insulin resistance in children and adolescents. *Pediatric Obesity* 2013; **8**(1): 52-61.

52. Wang TJ, Larson MG, Vasan RS, Cheng S, Rhee EP, McCabe E, Lewis GD, Fox CS, Jacques PF, Fernandez C, O'Donnell CJ, Carr SA, Mootha VK, Florez JC, Souza A, Melander O, Clish CB, Gerszten RE. Metabolite profiles and the risk of developing diabetes. *Nature Medicine* 2011; **17**(4): 448-U83.

53. Cummings NE, Williams EM, Kasza I, Konon EN, Schaid MD, Schmidt BA, Poudel C, Sherman DS, Yu DY, Apelo SIA, Cottrell SE, Geiger G, Barnes ME, Wisinski JA, Fenske RJ, Matkowskyj KA, Kimple ME, Alexander CM, Merrins MJ, Lamming DW. Restoration of metabolic health by decreased consumption of branched-chain amino acids. *J Physiol-London* 2018; **596**(4): 623-45.

54. Yu D, Richardson NE, Green CL, Spicer AB, Murphy ME, Flores V, Jang C, Kasza I, Nikodemova M, Wakai MH, Tomasiewicz JL, Yang SE, Miller BR, Pak HH, Brinkman JA, Rojas JM, Quinn WJ, 3rd, Cheng EP, Konon EN, Haider LR, Finke M, Sonsalla M, Alexander CM, Rabinowitz JD, Baur JA, Malecki KC, Lamming DW. The adverse metabolic effects of branched-chain amino acids are mediated by isoleucine and valine. *Cell Metab* 2021; **33**(5): 905-22 e6.

55. Jang C, Oh SF, Wada S, Rowe GC, Liu L, Chan MC, Rhee J, Hoshino A, Kim B, Ibrahim A, Baca LG, Kim E, Ghosh CC, Parikh SM, Jiang A, Chu Q, Forman DE, Lecker SH, Krishnaiah S, Rabinowitz JD, Weljie AM, Baur JA, Kasper DL, Arany Z. A branched-chain amino acid metabolite drives vascular fatty acid transport and causes insulin resistance. *Nat Med* 2016; **22**(4): 421-6.

56. Huffman KM, Shah Sh Fau - Stevens RD, Stevens Rd Fau - Bain JR, Bain Jr Fau - Muehlbauer M, Muehlbauer M Fau - Slentz CA, Slentz Ca Fau - Tanner CJ, Tanner Cj Fau - Kuchibhatla M, Kuchibhatla M Fau - Houmard JA, Houmard Ja Fau - Newgard CB, Newgard Cb Fau - Kraus WE, Kraus WE. Relationships between circulating metabolic intermediates and insulin action in overweight to obese, inactive men and women. *Diebetes* 2009; **32**(9): 1678-83.

57. Newgard CB. Interplay between lipids and branched-chain amino acids in development of insulin resistance. *Cell Metab* 2012; **15**(5): 606-14.

58. White PJ, McGarrah RW, Herman MA, Bain JR, Shah SH, Newgard CB. Insulin action, type 2 diabetes, and branched-chain amino acids: A two-way street. *Molecular Metabolism* 2021; **52**.

59. Manning BD. Balancing Akt with S6K: implications for both metabolic diseases and tumorigenesis. *J Cell Biol* 2004; **167**(3): 399-403.

60. Tremblay F, Krebs M, Dombrowski L, Brehm A, Bernroider E, Roth E, Nowotny P, Waldhausl W, Marette A, Roden M. Overactivation of S6 kinase 1 as a cause of human insulin resistance during increased amino acid availability. *Diabetes* 2005; **54**(9): 2674-84.

61. Yu YH, Yoon SO, Poulogiannis G, Yang Q, Ma XJM, Villen J, Kubica N, Hoffman GR, Cantley LC, Gygi SP, Blenis J. Phosphoproteomic Analysis Identifies Grb10 as an mTORC1 Substrate That Negatively Regulates Insulin Signaling. *Science* 2011; **332**(6035): 1322-6.

62. Huang EH, Hynes MJ, Zhang T, Ginestier C, Dontu G, Appelman H, Fields JZ, Wicha MS, Boman BM. Aldehyde dehydrogenase 1 is a marker for normal and malignant human colonic stem cells (SC) and tracks SC overpopulation during colon tumorigenesis. *Cancer Res* 2009; **69**(8): 3382-9.

63. Kedishvili NY, Popov KM, Rougraff PM, Zhao Y, Crabb DW, Harris RA. CoA-dependent methylmalonate-semialdehyde dehydrogenase, a unique member of the aldehyde dehydrogenase superfamily. cDNA cloning, evolutionary relationships, and tissue distribution. *J Biol Chem* 1992; **267**(27): 19724-9.

64. Pollitt RJ, Green A, Smith R. Excessive excretion of beta-alanine and of 3-hydroxypropionic, R- and S-3-aminoisobutyric, R- and S-3-hydroxyisobutyric and S-2-(hydroxymethyl)butyric acids probably due to a defect in the metabolism of the corresponding malonic semialdehydes. *J Inherit Metab Dis* 1985; **8**(2): 75-9.

65. Shield JP, Gough R, Allen J, Newbury-Ecob R. 3-Hydroxyisobutyric aciduria: phenotypic heterogeneity within a single family. *Clin Dysmorphol* 2001; **10**(3): 189-91.
66. Sass JO, Walter M, Shield JP, Atherton AM, Garg U, Scott D, Woods CG, Smith LD. 3-Hydroxyisobutyrate aciduria and mutations in the ALDH6A1 gene coding for methylmalonate semialdehyde dehydrogenase. *J Inherit Metab Dis* 2012; **35**(3): 437-42.
67. Marcadier JL, Smith AM, Pohl D, Schwartzentruber J, Al-Dirbashi OY, Consortium FC, Majewski J, Ferdinandusse S, Wanders RJ, Bulman DE, Boycott KM, Chakraborty P, Geraghty MT. Mutations in ALDH6A1 encoding methylmalonate semialdehyde dehydrogenase are associated with dysmyelination and transient methylmalonic aciduria. *Orphanet J Rare Dis* 2013; **8**: 98.
68. Dobrowolski SF, Alodaib A, Karunanidhi A, Basu S, Holecko M, Lichter-Konecki U, Pappan KL, Vockley J. Clinical, biochemical, mitochondrial, and metabolomic aspects of methylmalonate semialdehyde dehydrogenase deficiency: Report of a fifth case. *Mol Genet Metab* 2020; **129**(4): 272-7.
69. Nilsen MS, Jersin RA, Ulvik A, Madsen A, McCann A, Svensson PA, Svensson MK, Nedrebo BG, Gudbrandsen OA, Tell GS, Kahn CR, Ueland PM, Mellgren G, Dankel SN. 3-Hydroxyisobutyrate, A Strong Marker of Insulin Resistance in Type 2 Diabetes and Obesity That Modulates White and Brown Adipocyte Metabolism. *Diabetes* 2020; **69**(9): 1903-16.
70. Lyon ES, Rivera ME, Johnson MA, Sunderland KL, Vaughan RA. Actions of chronic physiological 3-hydroxyisobuterate treatment on mitochondrial metabolism and insulin signaling in myotubes. *Nutr Res* 2019; **66**: 22-31.
71. Roberts LD, Bostrom P, O'Sullivan JF, Schinzel RT, Lewis GD, Dejam A, Lee YK, Palma MJ, Calhoun S, Georgiadi A, Chen MH, Ramachandran VS, Larson MG, Bouchard C, Rankinen T, Souza AL, Clish CB, Wang TJ, Estall JL, Soukas AA, Cowan CA, Spiegelman BM, Gerszten RE. beta-Aminoisobutyric Acid Induces Browning of White Fat and Hepatic beta-Oxidation and Is Inversely Correlated with Cardiometabolic Risk Factors. *Cell Metab* 2014; **19**(1): 96-108.
72. Ko FJ, Nyhan WL, Wolff J, Barshop B, Sweetman L. 3-Hydroxyisobutyric Aciduria - an Inborn Error of Valine Metabolism. *Pediatr Res* 1991; **30**(4): 322-6.
73. Roe CR, Struys E Fau - Kok RM, Kok Rm Fau - Roe DS, Roe Ds Fau - Harris RA, Harris Ra Fau - Jakobs C, Jakobs C. Methylmalonic semialdehyde dehydrogenase deficiency: psychomotor delay and methylmalonic aciduria without metabolic decompensation. *Mol Genet Metab* 1998; **65**(1): 35-43.

74. Aghamaleki MA, Rezapour M, Babazadeh K, Zamani H, Aghajanpour F. Methylmalonate-Semialdehyde Dehydrogenase Deficiency With Cardiac Presentation: A Case Report With Literature Review. *J Pediat Rev* 2019; **7**(1): 55-9.

75. Dharuri H, t Hoen PA, van Klinken JB, Henneman P, Laros JF, Lips MA, El Bouazzaoui F, van Ommen GJ, Janssen I, van Ramshorst B, van Wagensveld BA, Pijl H, Willems van Dijk K, van Harmelen V. Downregulation of the acetyl-CoA metabolic network in adipose tissue of obese diabetic individuals and recovery after weight loss. *Diabetologia* 2014; **57**(11): 2384-92.

76. Moreno-Viedma V, Amor M, Sarabi A, Bilban M, Staffler G, Zeyda M, Stulnig TM. Common dysregulated pathways in obese adipose tissue and atherosclerosis. *Cardiovasc Diabetol* 2016; **15**(1): 120.

77. Timmons JA, Atherton PJ, Larsson O, Sood S, Blokhin IO, Brogan RJ, Volmar CH, Josse AR, Slentz C, Wahlestedt C, Phillips SM, Phillips BE, Gallagher IJ, Kraus WE. A coding and non-coding transcriptomic perspective on the genomics of human metabolic disease. *Nucleic Acids Res* 2018; **46**(15): 7772-92.

78. McCormack SE, Shaham O, McCarthy MA, Deik AA, Wang TJ, Gerszten RE, Clish CB, Mootha VK, Grinspoon SK, Fleischman A. Circulating branched-chain amino acid concentrations are associated with obesity and future insulin resistance in children and adolescents. *Pediatr Obes* 2013; **8**(1): 52-61.

79. Gannon NP, Schnuck JK, Vaughan RA. BCAA Metabolism and Insulin Sensitivity - Dysregulated by Metabolic Status? *Mol Nutr Food Res* 2018; **62**(6): e1700756.

80. Liu S, Cai XJ, Wang T, Xu JW, Cheng WL, Wang XL, Wei GJ, Yan S. Downregulation of ALDH6A1 is a New Marker of Muscle Insulin Resistance in Type 2 Diabetes Mellitus. *Int J Gen Med* 2022; **15**: 2137-47.

81. Shin H, Cha HJ, Lee MJ, Na K, Park D, Kim CY, Han DH, Kim H, Paik YK. Identification of ALDH6A1 as a Potential Molecular Signature in Hepatocellular Carcinoma via Quantitative Profiling of the Mitochondrial Proteome. *J Proteome Res* 2020; **19**(4): 1684-95.

82. Lu J, Chen Z, Zhao H, Dong H, Zhu L, Zhang Y, Wang J, Zhu H, Cui Q, Qi C, Wang S, Chen S, Shao J. ABAT and ALDH6A1, regulated by transcription factor HNF4A, suppress tumorigenic capability in clear cell renal cell carcinoma. *J Transl Med* 2020; **18**(1): 101.

83. Wang H, Dey KK, Chen PC, Li Y, Niu M, Cho JH, Wang X, Bai B, Jiao Y, Chepyala SR, Haroutunian V, Zhang B, Beach TG, Peng J. Integrated analysis of ultra-

deep proteomes in cortex, cerebrospinal fluid and serum reveals a mitochondrial signature in Alzheimer's disease. *Mol Neurodegener* 2020; **15**(1): 43.

84. Mauvais-Jarvis F, Arnold AP, Reue K. A Guide for the Design of Pre-clinical Studies on Sex Differences in Metabolism. *Cell Metab* 2017; **25**(6): 1216-30.

85. Moore MC, Cherrington AD, Wasserman DH. Regulation of hepatic and peripheral glucose disposal. *Best Pract Res Cl En* 2003; **17**(3): 343-64.

86. Lee HY, Jeong KH, Choi CS, International Mouse Phenotyping C. In-depth metabolic phenotyping of genetically engineered mouse models in obesity and diabetes. *Mamm Genome* 2014; **25**(9-10): 508-21.

87. Han SS, Kim KW, Kim KI, Na KY, Chae DW, Kim S, Chin HJ. Lean mass index: a better predictor of mortality than body mass index in elderly Asians. *J Am Geriatr Soc* 2010; **58**(2): 312-7.

88. Rui L. Brain regulation of energy balance and body weight. *Rev Endocr Metab Disord* 2013; **14**(4): 387-407.

89. Kaunitz H, Slanetz CA, Johnson RE, Guilmain J. Influence of Diet Composition on Caloric Requirements, Water Intake and Organ Weights of Rats during Restricted Food Intake. *J Nutr* 1956; **60**(2): 221-8.

90. Huang K, Huang Y Fau - Frankel J, Frankel J Fau - Addis C, Addis C Fau - Jaswani L, Jaswani L Fau - Wehner PS, Wehner Ps Fau - Mangiarua EI, Mangiarua Ei Fau - McCumbee WD, McCumbee WD. The short-term consumption of a moderately high-fat diet alters nitric oxide bioavailability in lean female Zucker rats. *Can JPhysiol Pharmacol* 2011; **89**(4): 245-57.

91. Volcko KL, Carroll QE, Brakey DJ, Daniels D. High-fat diet alters fluid intake without reducing sensitivity to glucagon-like peptide-1 receptor agonist effects. *Physiol Behav* 2020; **221**: 112910.

92. Kraly FS. Physiology of drinking elicited by eating. *Psychological Review* 1984; **91**(4): 478.

93. Boschmann M, Steiniger J, Hille U, Tank J, Adams F, Sharma AM, Klaus S, Luft FC, Jordan J. Water-Induced Thermogenesis. *The Journal of Clinical Endocrinology & Metabolism* 2003; **88**(12): 6015-9.

94. Brunkwall L, Ericson U, Nilsson PM, Enhörning S. High water intake and low urine osmolality are associated with favorable metabolic profile at a population level: low vasopressin secretion as a possible explanation. *European Journal of Nutrition* 2020; **59**(8): 3715-22.

95. Taveau C, Chollet C, Waeckel L, Desposito D, Bichet DG, Arthus M-F, Magnan C, Philippe E, Paradis V, Foufelle F, Hainault I, Enhorning S, Velho G, Roussel R, Bankir L, Melander O, Bouby N. Vasopressin and hydration play a major role in the development of glucose intolerance and hepatic steatosis in obese rats. *Diabetologia* 2015; **58**(5): 1081-90.

96. Liu S, Sun Y, Zhao R, Wang Y, Zhang W, Pang W. Isoleucine increases muscle mass through promoting myogenesis and intramyocellular fat deposition. *Food Funct* 2021; **12**(1): 144-53.

97. Duan Y, Li F, Li Y, Tang Y, Kong X, Feng Z, Anthony TG, Watford M, Hou Y, Wu G, Yin Y. The role of leucine and its metabolites in protein and energy metabolism. *Amino Acids* 2016; **48**(1): 41-51.

98. Hill JO, Wyatt HR, Peters JC. Energy balance and obesity. *Circulation* 2012; **126**(1): 126-32.

99. Du Y, Meng Q, Zhang Q, Guo F. Isoleucine or valine deprivation stimulates fat loss via increasing energy expenditure and regulating lipid metabolism in WAT. *Amino Acids* 2012; **43**(2): 725-34.

100. Zapata RC, Singh A, Pezeshki A, Avirineni BS, Patra S, Chelikani PK. Low-Protein Diets with Fixed Carbohydrate Content Promote Hyperphagia and Sympathetically Mediated Increase in Energy Expenditure. *Mol Nutr Food Res* 2019; **63**(21): e1900088.

101. Yu DY, Richardson NE, Green CL, Spicer AB, Murphy ME, Flores V, Jang C, Kasza I, Nikodemova M, Wakai MH, Tomasiewicz JL, Yang SE, Miller BR, Pak HH, Brinkman JA, Rojas JM, Quinn WJ, Cheng EP, Konon EN, Haider LR, Finke M, Sonsalla M, Alexander CM, Rabinowitz JD, Baur JA, Malecki KC, Lamming DW. The adverse metabolic effects of branched-chain amino acids are mediated by isoleucine and valine. *Cell Metabolism* 2021; **33**(5): 905-+.

102. Yuan FX, Jiang HZ, Yin HR, Jiang XX, Jiao FX, Chen SH, Ying H, Chen Y, Zhai QW, Guo FF. Activation of GCN2/ATF4 signals in amygdalar PKC-delta neurons promotes WAT browning under leucine deprivation. *Nat Commun* 2020; **11**(1).

103. Marcadier JL, Smith AM, Pohl D, Schwartzentruber J, Al-Dirbashi OY, Majewski J, Ferdinandusse S, Wanders RJ, Bulman DE, Boycott KM, Chakraborty P, Geraghty MT. Mutations in ALDH6A1 encoding methylmalonate semialdehyde dehydrogenase are associated with dysmyelination and transient methylmalonic aciduria. *Orphanet J Rare Dis* 2013; **8**: 98.

104. Bjune MS, Lindquist C, Hallvardsdotter Stafsnes M, Bjørndal B, Bruheim P, Aloysius TA, Nygård O, Skorve J, Madsen L, Dankel SN, Berge RK. Plasma 3-hydroxyisobutyrate (3-HIB) and methylmalonic acid (MMA) are markers of hepatic mitochondrial fatty acid oxidation in male Wistar rats. *Biochimica et Biophysica Acta (BBA) - Molecular and Cell Biology of Lipids* 2021; **1866**(4): 158887.

105. Nilsen MS, Jersin R, Ulvik A, Madsen A, McCann A, Svensson PA, Svensson MK, Nedrebø BG, Gudbrandsen OA, Tell GS, Kahn CR, Ueland PM, Mellgren G, Dankel SN. 3-Hydroxyisobutyrate, A Strong Marker of Insulin Resistance in Type 2 Diabetes and Obesity That Modulates White and Brown Adipocyte Metabolism. *Diabetes* 2020; **69**(9): 1903-16.

106. Timmons JA, Atherton PJ, Larsson O, Sood S, Blokhin IO, Brogan RJ, Volmar CH, Josse AR, Slentz C, Wahlestedt C, Phillips SM, Phillips BE, Gallagher IJ, Kraus WE. A coding and non-coding transcriptomic perspective on the genomics of human metabolic disease. *Nucleic Acids Research* 2018; **46**(15): 7772-92.

107. Shimba Y, Togawa H, Senoo N, Ikeda M, Miyoshi N, Morita A, Miura S. Skeletal Muscle-specific PGC-1α Overexpression Suppresses Atherosclerosis in Apolipoprotein E-Knockout Mice. *Sci Rep* 2019; **9**(1): 4077.

108. Roberts LD, Boström P, O'Sullivan JF, Schinzel RT, Lewis GD, Dejam A, Lee YK, Palma MJ, Calhoun S, Georgiadi A, Chen MH, Ramachandran VS, Larson MG, Bouchard C, Rankinen T, Souza AL, Clish CB, Wang TJ, Estall JL, Soukas AA, Cowan CA, Spiegelman BM, Gerszten RE. β-Aminoisobutyric acid induces browning of white fat and hepatic β-oxidation and is inversely correlated with cardiometabolic risk factors. *cell Metab* 2014; **19**(1): 96-108.

Statutory Declaration

“I, Rongwan Sun, by personally signing this document in lieu of an oath, hereby affirm that I prepared the submitted dissertation on the topic Metabolic characterization and molecular alteration of *Aldh6a1*-deficient mice during diet-induced obesity / Metabolische Charakterisierung und molekulare Veränderung *Aldh6a1*-defizienter Mäuse unter diätinduzierter Adipositas, independently and without the support of third parties, and that I used no other sources and aids than those stated.
All parts which are based on the publications or presentations of other authors, either in letter or in spirit, are specified as such in accordance with the citing guidelines. The sections on methodology (in particular regarding practical work, laboratory regulations, statistical processing) and results (in particular regarding figures, charts and tables) are exclusively my responsibility.

Furthermore, I declare that I have correctly marked all of the data, the analyses, and the conclusions generated from data obtained in collaboration with other persons, and that I have correctly marked my own contribution and the contributions of other persons (cf. declaration of contribution). I have correctly marked all texts or parts of texts that were generated in collaboration with other persons.

My contributions to any publications to this dissertation correspond to those stated in the below joint declaration made together with the supervisor. All publications created within the scope of the dissertation comply with the guidelines of the ICMJE (International Committee of Medical Journal Editors; http://www.icmje.org) on authorship. In addition, I declare that I shall comply with the regulations of Charité – Universitätsmedizin Berlin on ensuring good scientific practice.

I declare that I have not yet submitted this dissertation in identical or similar form to another Faculty.

The significance of this statutory declaration and the consequences of a false statutory declaration under criminal law (Sections 156, 161 of the German Criminal Code) are known to me.”

Date Signature

Curriculum Vitae

My curriculum vitae does not appear in the electronic version of my paper for reasons of data protection

Acknowledgements

During the period of my research, I felt grateful for the support of my first supervisor Prof. Dr. Joachim Spranger and my second supervisor Dr. Sebastian Brachs, they provide an opportunity to study this project and pursuit a doctorate degree at Charite University. I had a real nice time with our team at Endocrinology, Diabetes and Nutrition department in the past years. At the same time, I would like to thank “Chinese Scholar Council” for providing me with financial support to complete the project abroad.

I would like to express my gratitude to Dr. Sebastian Brachs, who broaden my knowledge and made me have an intact scientific mind. I appreciate his vast knowledge and skills in the metabolism area, and it really gives me much more help and good suggestions. I also thank Dr. Eva Katrin Wirth, she sometimes gives me good advice.

I would thank our team’s help, including Diana Woellner, Marie-Christin Gaerz, Nadine Huckauf. They not only taught me a lot of experimental techniques used in the project but also helped me solve laboratory problems. Many thanks to my colleague, Dr.med Aoxue Liu, Dr.med Aida Harutyunyan, Dr.med Olena Mackert, for their accompany and assistance.

Last but not least, I would further to thank my family Yue Xu and my parents for constant encouragement and love in my hardest time. I also thank my friends-Yuanyuan Zhai, Zhengzheng He, Qing Li, Tong Liu, they give me kind help and motivation in every day!

Confirmation by a statistician

CHARITÉ

CharitéCentrum für Human- und Gesundheitswissenschaften

Charité | Campus Charité Mitte | 10117 Berlin

Name, Vorname: Sun, Rongwan
Emailadresse: rongwan.sun@charite.de
Matrikelnummer: 226220
Promotionsbetreuerin: Prof. Dr. Joachim Spranger
Promotionsinstitution / Klinik: Department of Endocrinology and Metabolism Cardiovascular Metabolic Renal Research Center (CMR)

Institut für Biometrie und klinische Epidemiologie (iBikE)
Direktor: Prof. Dr. Frank Konietschke
Postanschrift:
Charitéplatz 1 | 10117 Berlin
Besucheranschrift:
Reinhardtstr. 58 | 10117 Berlin
Tel. +49 (0)30 450 562171
geraldine.rauch@charite.de
https://biometrie.charite.de/

Bescheinigung

Hiermit bescheinige ich, dass Frau *Rongwan Sun* innerhalb der Service Unit Biometrie des Instituts für Biometrie und klinische Epidemiologie (iBikE) bei mir eine statistische Beratung zu einem Promotionsvorhaben wahrgenommen hat. Folgende Beratungstermine wurden wahrgenommen:

- Termin 1: *03.02.2022*

Folgende wesentliche Ratschläge hinsichtlich einer sinnvollen Auswertung und Interpretation der Daten wurden während der Beratung erteilt:

- Überprüfung der Normalverteilung
- Two-way ANOVA
- Effektgröße
- Korrektur für multiples Testen

Diese Bescheinigung garantiert nicht die richtige Umsetzung der in der Beratung gemachten Vorschläge, die korrekte Durchführung der empfohlenen statistischen Verfahren und die richtige Darstellung und Interpretation der Ergebnisse. Die Verantwortung hierfür obliegt allein dem Promovierenden. Das Institut für Biometrie und klinische Epidemiologie übernimmt hierfür keine Haftung.

Datum: 31.05.2022

Name des Beraters/der Beraterin: Pimrapat Gebert

Unterschrift Beraterin, Institutsstempel

CHARITÉ
UNIVERSITÄTSMEDIZIN BERLIN
Institut für Biometrie und Klinische Epidemiologie
Campus Charité Mitte
Charitéplatz 1 | D-10117 Berlin
Sitz: Reinhardtstr. 58